Cooperative Simultaneous Localization and Synchronization in Mobile Agent Networks

Bernhard Etzlinger, *Member, IEEE*, Florian Meyer, *Member, IEEE*, Franz Hlawatsch, *Fellow, IEEE*, Andreas Springer, *Member, IEEE*, and Henk Wymeersch, *Member, IEEE*

***Abstract*—Cooperative localization in agent networks based on interagent time-of-flight measurements is closely related to synchronization. To leverage this relation, we propose a Bayesian factor graph framework for *cooperative simultaneous localization and synchronization* (CoSLAS). This framework is suited to mobile agents and time-varying local clock parameters. Building on the CoSLAS factor graph, we develop a distributed (decentralized) belief propagation algorithm for CoSLAS in the practically important case of an affine clock model and asymmetric time stamping. Our algorithm is compatible with real-time operation and a time-varying network connectivity. To achieve high accuracy at reduced complexity and communication cost, the algorithm combines particle implementations with parametric message representations and takes advantage of a conditional independence property. Simulation results demonstrate the good performance of the proposed algorithm in a challenging scenario with time-varying network connectivity.**

***Index Terms*—Agent network, network synchronization, cooperative localization, belief propagation, message passing, factor graph, CoSLAS.**

I. Introduction

A. Background and State of the Art

Location information in agent networks enables a multitude of location-aware applications [1]–[4]. In many systems, the location information is obtained from interagent time measurements: each interagent distance is related to the time-of-flight of a signal and can thus be estimated from time-of-arrival measurements, and the agent locations can then be estimated in a distributed (decentralized) manner via cooperative localization techniques [5]. This scheme presupposes a common time base at all the agents and, thus, accurate synchronization throughout the network. Accordingly, several methods for *simultaneous localization and synchronization* (SLAS) have been developed recently. These methods can be classified into six groups as follows. Estimation of static clock and location parameters is considered (i) for a single agent in [6]–[9], (ii) for multiple agents with centralized computation in [10]–[12], and (iii) for multiple agents with distributed computation in [12]–[16]. For a single agent, (iv) estimation of dynamic clock parameters and static location parameters is considered in [17], and (v) estimation of static clock parameters and dynamic location parameters is considered in [18]. (vi) Distributed estimation of dynamic clock and location parameters of multiple agents is considered in [19].

Hereafter, we consider only *distributed* SLAS methods for *multiple* agents, i.e., methods from groups (iii) and (vi). In these methods, the local clocks differ either only in a clock offset [12], [16], [19] or in both a clock offset and a clock skew [13]–[15]. Considering also clock skews is important for accurate localization when multiple time measurements are combined for each communication link [20].

To account for the nonlinear measurement model of the SLAS problem, the distributed methods mentioned above use distributed least-squares (LS) or maximum likelihood estimation methods [12], [13] or Bayesian message passing methods [14]–[16], [19]. Typically, message passing methods require significantly fewer iterations than distributed LS methods [12]–[14]. Despite this advantage, to the best of our knowledge, only [19] previously proposed the message passing approach for SLAS in mobile, dynamic agent networks. However, the method in [19] is limited in practical scenarios in that no clock skews are considered, spatial references (anchors) must also serve as temporal references, and a linearization of the likelihood function is used that presupposes a dense deployment of anchors in the network.

Bayesian message passing methods are a powerful approach to cooperative estimation in agent networks and have been widely used for cooperative localization and cooperative synchronization individually [21]–[27]. To deal with nonlinearities in the message passing schemes, [14] and [15] use particle representations of messages whereas [16] and [19] use Gaussian messages based on the linearization of a specific term in the likelihood function. The particle-based methods outperform the linearized Gaussian method if only few agents with a spatial reference are available; this comes at the cost of higher communication requirements. In cooperative localization, the communication requirements of message passing can be reduced by using a parametric message approximation [23] or a sigma point implementation [24]. In cooperative

First revision, Januray 27, 2017; accepted March 2, 2017.

B. Etzlinger and A. Springer are with the Institute for Communications Engineering and RF-Systems, Johannes Kepler University, Linz, Austria (email:{bernhard.etzlinger,andreas.springer}@jku.at). F. Meyer is with the Laboratory for Information and Decision Systems, Massachusetts Institute of Technology, Cambridge, MA, USA (e-mail: fmeyer@mit.edu) and on leave of absence from the Centre for Maritime Research and Experimentation (CMRE), La Spezia, Italy. F. Hlawatsch is with the Institute of Telecommunications, TU Wien, Vienna, Austria (email: franz.hlawatsch@tuwien.ac.at). H. Wymeersch is with the Department of Signals and Systems, Chalmers University of Technology, Gothenburg, Sweden (email: henk.wymeersch@ieee.org). This work was supported in part by the Linz Center of Mechatronics (LCM) in the framework of the Austrian COMET-K2 programme, by the NATO Supreme Allied Command Transformation under project SAC000601, by the FWF under grants S10603-N13, P27370-N30, and J3886-N31, by the Newcom# Network of Excellence in Wireless Communications of the European Commission, by the Czech National Sustainability Programme under grant LO1401, by the European Research Council under grant 258418 (COOPNET), and by the EU HIGHTS project MG-3.5a-2014-636537. Parts of this work were previously presented at the 47th Asilomar Conference on Signals, Systems and Computers, Pacific Grove, CA, USA, Nov. 2013.

synchronization, Gaussian messages can be used because the measurement equations are approximately linear [26].

B. Contributions and Paper Organization

Here, we present a unified belief propagation (BP) message passing framework and algorithm for distributed *cooperative SLAS* (CoSLAS) in mobile agent networks with time-varying local clocks. BP methods provide accurate and computationally efficient solutions in many applications [21]–[30]. In the proposed BP framework, a low dimension of the involved state variables is achieved by exploiting the conditional independence of time measurements and location-related parameters given the interagent distances, which leads to a detailed factorization of the joint posterior probability density function (pdf). In this factorization, the dimension of the state variables does not depend on the number of agents in the network, thus yielding excellent scalability.

The proposed BP algorithm enables each agent to determine its own clock and location parameters in a distributed, cooperative, sequential manner. The algorithm is a hybrid—both particle-based and parametric—implementation of BP that relies on a practically relevant model for the clocks, state evolutions, and measurements. This model supports parametric representations of all messages, which strongly reduces computation and communication requirements compared to purely particle-based methods [15]. The algorithm extends state-of-the-art methods in that it is suited to time-varying clock and location parameters, time-varying network connectivity, and networks where the sets of spatial and temporal reference agents may be different or even disjoint.

This paper is organized as follows. The agent network, clock model, and state evolution model are described in Section II. The measurement model and corresponding likelihood function are developed in Section III. In Section IV, we present a "low-dimensional" factorization of the joint posterior pdf and the corresponding factor graph, and we review the BP scheme for approximate marginalization. The parametric message representations used by our algorithm are described in Section V. Section VI develops the proposed CoSLAS algorithm. Finally, Section VII presents simulation results.

This paper advances beyond the results reported in our conference publication [15] in that (i) it extends the CoSLAS factor graph framework and BP message passing algorithm of [15] to a time-dependent scenario and a sequential (time-recursive) operation; (ii) it presents a BP algorithm for mobile agents with time-varying local clocks; (iii) it proposes parametric representations for all messages.

C. Notation

We denote vectors by boldface lower-case characters (e.g., $\mathbf{x}$), matrices by boldface upper-case characters (e.g., $\mathbf{X}$), and sets by calligraphic upper-case characters (e.g., $\mathcal{X}$). The kth element of a vector is denoted by $[\cdot]_k$, and the (k,l)th element of a matrix by $[\cdot]_{k,l}$. We write i (and, occasionally, j) for the index of an agent, n for the discrete time index, k for the index of a packet transmission, s (and, occasionally, r) for the index of a mixture component, l for the index of a particle, and q for the index of a message passing iteration. The numbers of agents, packet transmissions, mixture components, particles, and message passing iterations are accordingly denoted by I, K, S, L, and Q, respectively. The shorthand $\mathcal{N}(\mathbf{x};\boldsymbol{\mu},\boldsymbol{\Sigma})$ denotes a Gaussian pdf $f(\mathbf{x})$ with mean vector $\boldsymbol{\mu}$ and covariance matrix $\boldsymbol{\Sigma}$. The symbol $\propto$ indicates equality up to a constant factor, and the symbol $\sim$ indicates the distribution of a random variable.

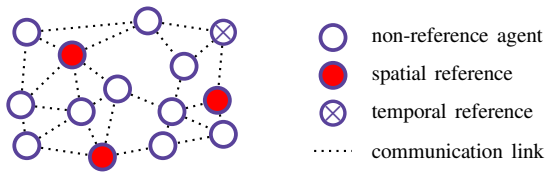

Fig. 1. Exemplary agent network, in which three agents are spatial references and one agent is a temporal reference.

II. Network and States

A. Agent Network, Clock Model, and States

We consider a connected time-varying network of I mobile, asynchronous agents $i \in \mathcal{I} \triangleq \{1,\ldots,I\}$. The reference time, t, is slotted into intervals $[nT,(n+1)T)$, $n \in \{0,1,\ldots\}$. The agents know the interval duration T but, due to their imprecise clocks, are not able to autonomously determine the beginning of a new time interval. At time step n, i.e., during the nth time interval, two agents $i,j \in \mathcal{I}$, $i \neq j$ are able to communicate if $(i,j) \in \mathcal{C}^{(n)} \subseteq \mathcal{I}\times\mathcal{I}$ (and, by symmetry, $(j,i) \in \mathcal{C}^{(n)}$). The *neighborhood* $\mathcal{T}_i^{(n)} \subseteq \mathcal{I}\setminus\{i\}$ of agent $i \in \mathcal{I}$ consists of all agents $j \in \mathcal{I}\setminus\{i\}$ that communicate with agent i at time step n, i.e., $\mathcal{T}_i^{(n)} \triangleq \big\{j \in \mathcal{I}\setminus\{i\} \,\big|\, (i,j) \in \mathcal{C}^{(n)}\big\}$. Note that $\mathcal{C}^{(n)}$ and $\mathcal{T}^{(n)}$ are assumed constant within the nth time interval. Some of the agents i are spatial and/or temporal references, which have perfect knowledge of their own location and/or clock, respectively, at all times. In particular, a temporal reference agent is able to determine the beginning of a new time interval. An example of such an agent network is depicted in Fig. 1.

Each agent $i \in \mathcal{I}$ has an internal/local clock c_i, whose dependence on the reference time t is modeled as

$$c_i\big(t;\boldsymbol{\vartheta}_i^{(n)}\big) = \alpha_i^{(n)} t + \beta_i^{(n)}. \tag{1}$$

Here, $\alpha_i^{(n)} > 0$ and $\beta_i^{(n)} \in \mathbb{R}$ are the *clock skew* and *clock phase*, respectively, which define the *clock state* $\boldsymbol{\vartheta}_i^{(n)} \triangleq \big[\nu_i^{(n)}\ \lambda_i^{(n)}\big]^{\mathrm{T}}$ with $\nu_i^{(n)} \triangleq \beta_i^{(n)}/\alpha_i^{(n)}$ and $\lambda_i^{(n)} \triangleq 1/\alpha_i^{(n)}$. (This parameter transformation leads to an approximately Gaussian likelihood function, cf. Section III-B.) Each agent i has a *location-related state* $\mathbf{x}_i^{(n)} \triangleq \big[\mathbf{p}_i^{(n)\mathrm{T}}\ \dot{\mathbf{p}}_i^{(n)\mathrm{T}}\big]^{\mathrm{T}}$, where $\mathbf{p}_i^{(n)} \triangleq \big[x_{1,i}^{(n)}\ x_{2,i}^{(n)}\big]^{\mathrm{T}}$ is the location vector and $\dot{\mathbf{p}}_i^{(n)} \triangleq \big[\dot{x}_{1,i}^{(n)}\ \dot{x}_{2,i}^{(n)}\big]^{\mathrm{T}}$ is the velocity vector (relative to t). The *state* of agent i at time step n is thus given by $\boldsymbol{\theta}_i^{(n)} \triangleq \big[\boldsymbol{\vartheta}_i^{(n)\mathrm{T}}\ \mathbf{x}_i^{(n)\mathrm{T}}\big]^{\mathrm{T}}$. We note that $\mathbf{p}_i^{(n)} = \mathbf{P}\mathbf{x}_i^{(n)}$ with $\mathbf{P} = \big[\mathbf{I}_2\ \mathbf{0}_2\big]$, where $\mathbf{I}_2$ is the 2×2 identity matrix and $\mathbf{0}_2$ is the 2×2 zero matrix.

B. State-Evolution Model and Prior Distribution

For the temporal evolution of the clock state $\boldsymbol{\vartheta}_i^{(n)}$, we use a standard random walk model as in [17], i.e.,

$$\boldsymbol{\vartheta}_i^{(n)} = \boldsymbol{\vartheta}_i^{(n-1)} + \mathbf{u}_{1,i}^{(n)}, \qquad n = 1, 2, \dots, \tag{2}$$

where $\mathbf{u}_{1,i}^{(n)} \sim \mathcal{N}\big(\mathbf{u}_{1,i}^{(n)}; \mathbf{0}, \boldsymbol{\Sigma}_{u_{1,i}}\big)$ with $\boldsymbol{\Sigma}_{u_{1,i}} = \operatorname{diag}\big\{\sigma_{1,i}^2, \sigma_{2,i}^2\big\}$ is Gaussian process noise that is independent across n and i. The state-evolution pdf corresponding to (2) is

$$f\big(\boldsymbol{\vartheta}_i^{(n)} \big| \boldsymbol{\vartheta}_i^{(n-1)}\big) \propto \exp\left(-\frac{1}{2}\big\|\boldsymbol{\vartheta}_i^{(n)} - \boldsymbol{\vartheta}_i^{(n-1)}\big\|^2_{\boldsymbol{\Sigma}_{u_{1,i}}^{-1}}\right),$$

where $\|\mathbf{u}\|^2_{\mathbf{A}} \triangleq \mathbf{u}^{\mathrm{T}}\mathbf{A}\mathbf{u}$. The temporal evolution of the location-related state $\mathbf{x}_i^{(n)}$ is modeled as [31]

$$\mathbf{x}_i^{(n)} = \mathbf{G}_1 \mathbf{x}_i^{(n-1)} + \mathbf{u}_{2,i}^{(n)}, \qquad n = 1, 2, \dots, \tag{3}$$

where $\mathbf{u}_{2,i}^{(n)} \sim \mathcal{N}\big(\mathbf{u}_{2,i}^{(n)}; \mathbf{0}, \boldsymbol{\Sigma}_{u_{2,i}}\big)$ with $\boldsymbol{\Sigma}_{u_{2,i}} = \sigma_{u_{2,i}}^2 \mathbf{G}_2 \mathbf{G}_2^{\mathrm{T}}$; here, $\mathbf{G}_1$ and $\mathbf{G}_2$ are as in [31], i.e.,

$$\mathbf{G}_1 = \begin{bmatrix} 1 & 0 & T & 0 \\ 0 & 1 & 0 & T \\ 0 & 0 & 1 & 0 \\ 0 & 0 & 0 & 1 \end{bmatrix}, \quad \mathbf{G}_2 = \begin{bmatrix} T^2/2 & 0 \\ 0 & T^2/2 \\ T & 0 \\ 0 & T \end{bmatrix}.$$

The state-evolution pdf corresponding to (3) is

$$f\big(\mathbf{x}_i^{(n)} \big| \mathbf{x}_i^{(n-1)}\big) \propto \exp\left(-\frac{1}{2}\big\|\mathbf{x}_i^{(n)} - \mathbf{G}_1 \mathbf{x}_i^{(n-1)}\big\|^2_{\boldsymbol{\Sigma}_{u_{2,i}}^{-1}}\right).$$

Furthermore, $\mathbf{u}_{1,i}^{(n)}$ and $\mathbf{u}_{2,i}^{(n)}$ are assumed independent and also independent across i and n. The initial states $\boldsymbol{\vartheta}_i^{(0)}$ and $\mathbf{x}_i^{(0)}$ are modeled as independent, independent across i, and Gaussian with independent entries, i.e.,

$$\boldsymbol{\vartheta}_i^{(0)} \sim f\big(\boldsymbol{\vartheta}_i^{(0)}\big) = \mathcal{N}\big(\boldsymbol{\vartheta}_i^{(0)}; \boldsymbol{\mu}_{f_i \to \vartheta_i}^{(0)}, \boldsymbol{\Sigma}_{f_i \to \vartheta_i}^{(0)}\big), \tag{4}$$

$$\mathbf{x}_i^{(0)} \sim f\big(\mathbf{x}_i^{(0)}\big) = \mathcal{N}\big(\mathbf{x}_i^{(0)}; \boldsymbol{\mu}_{l_i \to x_i}^{(0)}, \boldsymbol{\Sigma}_{l_i \to x_i}^{(0)}\big), \tag{5}$$

with $\boldsymbol{\Sigma}_{f_i \to \vartheta_i}^{(0)} = \operatorname{diag}\big\{\sigma_{\nu_i}^2, \sigma_{\lambda_i}^2\big\}$ and $\boldsymbol{\Sigma}_{l_i \to x_i}^{(0)} = \operatorname{diag}\big\{\sigma_{x_i}^2, \sigma_{\dot{x}_i}^2, \sigma_{\dot{x}_i}^2, \sigma_{\dot{x}_i}^2\big\}$. It follows that the joint prior pdf of all the states up to time n factors as

$$f\big(\boldsymbol{\theta}^{(0:n)}\big) = \prod_{i \in \mathcal{I}} f\big(\boldsymbol{\vartheta}_i^{(0)}\big) f\big(\mathbf{x}_i^{(0)}\big) \times \prod_{n'=1}^{n} f\big(\boldsymbol{\vartheta}_i^{(n')} \big| \boldsymbol{\vartheta}_i^{(n'-1)}\big)\, f\big(\mathbf{x}_i^{(n')} \big| \mathbf{x}_i^{(n'-1)}\big). \tag{6}$$

Here, $\boldsymbol{\theta}^{(0:n)}$ collects all $\boldsymbol{\theta}_i^{(n')}$ for $i \in \mathcal{I}$ and $n' \in \{0, \dots, n\}$.

III. Measurements and Likelihood Function

A. Time-Stamping Measurement Model

Each time interval $[nT, (n+1)T)$ contains a "measurement phase" in which the agents acquire measurements. Each measurement phase consists of an *initialization* in which the temporal reference agents inform the other agents about the beginning of the measurement phase, and a *packet exchange* during which the agents obtain time measurements using the asymmetric time-stamped communication scheme proposed in [32]. The measurement phase is short compared to the time interval duration T, so that the clock parameters are approximately constant during the measurement phase.

1. Initialization: The agents are not able to determine autonomously the start of a new time interval and, in turn, of a packet exchange. This information is provided by the temporal reference agents via the following protocol: (i) After time T has passed since the beginning of the last measurement phase, each temporal reference agent initializes a new time interval by broadcasting a "start packet exchange" message to its neighbors. (ii) When an agent receives a "start packet exchange" message from one of its neighbors, it starts the packet exchange with that neighbor and itself broadcasts a "start packet exchange" message to its neighbors.

2. Packet exchange: Consider a communicating agent pair $(i, j) \in \mathcal{C}^{(n)}$ with distance $\big\|\mathbf{p}_i^{(n)} - \mathbf{p}_j^{(n)}\big\|$. Agent i transmits $K_{ij} \geq 1$ packets to agent j, and agent j transmits $K_{ji} \geq 1$ packets to agent i. The communication is termed asymmetric if $K_{ij} \neq K_{ji}$ in general [7]. At time $n \geq 1$, the kth "$i \to j$" packet (where $k \in \{1, \dots, K_{ij}\}$) departs from agent i at time $s_{ij}^{(n,k)}$ and arrives at agent j at measured time

$$r_{ij}^{(n,k)} = s_{ij}^{(n,k)} + \delta_{ij}^{(n,k)}, \text{ with } \delta_{ij}^{(n,k)} \triangleq \frac{\|\mathbf{p}_i^{(n)} - \mathbf{p}_j^{(n)}\|}{c} + v_{ij}^{(n,k)}. \tag{7}$$

Here, $\delta_{ij}^{(n,k)}$ is the delay expressed in true time, c is the speed of light, and $v_{ij}^{(n,k)} \sim \mathcal{N}\big(v_{ij}^{(n,k)}; 0, \sigma_v^2\big)$ is Gaussian measurement noise that is independent and identically distributed (iid) across i, j, k, and n. The transmit times $s_{ij}^{(n,k)}$ and receive times $r_{ij}^{(n,k)}$ are recorded at agent i and j, respectively in local time according to (1). This results in the *time stamps*

$$c_i\big(s_{ij}^{(n,k)}\big) = \alpha_i^{(n)} s_{ij}^{(n,k)} + \beta_i^{(n)}, \tag{8}$$

$$c_j\big(r_{ij}^{(n,k)}\big) = \alpha_j^{(n)} r_{ij}^{(n,k)} + \beta_j^{(n)}. \tag{9}$$

Plugging (7) into (9) and inserting in the resulting expression the expression of $s_{ij}^{(n,k)}$ obtained from (8), we find

$$c_j\big(r_{ij}^{(n,k)}\big) = \psi_{i \to j}^{(n,k)}\big(\boldsymbol{\theta}_i^{(n)}, \boldsymbol{\theta}_j^{(n)}\big) + v_{ij}^{(n,k)} \alpha_j^{(n)}, \tag{10}$$

with

$$\psi_{i \to j}^{(n,k)}\big(\boldsymbol{\theta}_i^{(n)}, \boldsymbol{\theta}_j^{(n)}\big) \triangleq \left(\frac{c_i\big(s_{ij}^{(n,k)}\big) - \beta_i^{(n)}}{\alpha_i^{(n)}} + \frac{\|\mathbf{p}_i^{(n)} - \mathbf{p}_j^{(n)}\|}{c}\right)\alpha_j^{(n)} + \beta_j^{(n)}. \tag{11}$$

Similarly, the transmission of the kth packet from agent j to agent i (where $k \in \{1, \dots, K_{ji}\}$) yields the time stamps $c_j\big(s_{ji}^{(n,k)}\big)$ and $c_i\big(r_{ji}^{(n,k)}\big)$; expressions of these time stamps are obtained by exchanging i and j in (8)–(11). The clock functions $c_i\big(t; \boldsymbol{\vartheta}_i^{(n)}\big)$ and $c_j\big(t; \boldsymbol{\vartheta}_j^{(n)}\big)$ and time stamps are visualized in Fig. 2. A communication protocol ensures that these time stamps are available at both agents i and j.

The aggregated measurement of agents i and j comprises all "received" time stamps, i.e., $\mathbf{y}_{ij}^{(n)} \triangleq \big[\mathbf{y}_{i \to j}^{(n)\mathrm{T}}\ \mathbf{y}_{j \to i}^{(n)\mathrm{T}}\big]^{\mathrm{T}}$ with $\mathbf{y}_{i \to j}^{(n)} \triangleq \big[c_j\big(r_{ij}^{(n,1)}\big) \cdots c_j\big(r_{ij}^{(n,K_{ij})}\big)\big]^{\mathrm{T}}$ and $\mathbf{y}_{j \to i}^{(n)} \triangleq \big[c_i\big(r_{ji}^{(n,1)}\big) \cdots c_i\big(r_{ji}^{(n,K_{ji})}\big)\big]^{\mathrm{T}}$. We also define the (recorded, not measured) "transmitted" time stamp vectors $\tilde{\mathbf{y}}_{i \to j}^{(n)} \triangleq \big[c_i\big(s_{ij}^{(n,1)}\big) \cdots c_i\big(s_{ij}^{(n,K_{ij})}\big)\big]^{\mathrm{T}}$ and $\tilde{\mathbf{y}}_{j \to i}^{(n)} \triangleq \big[c_j\big(s_{ji}^{(n,1)}\big) \cdots c_j\big(s_{ji}^{(n,K_{ji})}\big)\big]^{\mathrm{T}}$.

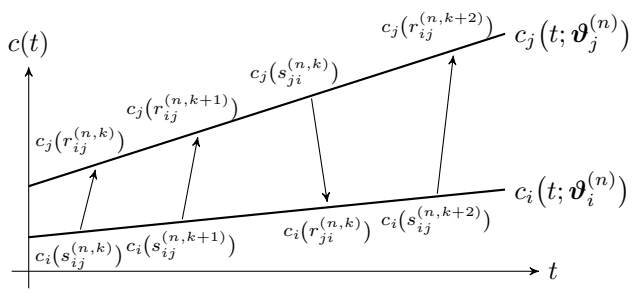

Fig. 2. Local clock functions $c_i\big(t,\boldsymbol{\vartheta}_i^{(n)}\big)$ and $c_j\big(t,\boldsymbol{\vartheta}_j^{(n)}\big)$, packet transmissions, and local time measurements (time stamps) for agents i and j.

B. Likelihood Function

We first consider the "single-packet" likelihood function of the kth $i\to j$ packet at time n, $f\big(c_j\big(r_{ij}^{(n,k)}\big)\big|\boldsymbol{\theta}_i^{(n)},\boldsymbol{\theta}_j^{(n)}\big)$. From (10) with $v_{ij}^{(n,k)}\sim\mathcal{N}\big(v_{ij}^{(n,k)};0,\sigma_v^2\big)$, we obtain

$$f\big(c_j\big(r_{ij}^{(n,k)}\big)\big|\boldsymbol{\theta}_i^{(n)},\boldsymbol{\theta}_j^{(n)}\big) = \frac{1}{\sqrt{2\pi}\alpha_j^{(n)}\sigma_v}\exp\left(-\frac{\Big(c_j\big(r_{ij}^{(n,k)}\big)-\psi_{i\to j}^{(n,k)}\big(\boldsymbol{\theta}_i^{(n)},\boldsymbol{\theta}_j^{(n)}\big)\Big)^2}{2\alpha_j^{(n)2}\sigma_v^2}\right).$$

The single-packet likelihood function for the kth $j\to i$ packet, $f\big(c_i\big(r_{ji}^{(n,k)}\big)\big|\boldsymbol{\theta}_i^{(n)},\boldsymbol{\theta}_j^{(n)}\big)$, is obtained by exchanging i and j. Because $v_{ij}^{(n,k)}$ was assumed iid across i, j, and k, the measurements between any agents i and j with $(i,j)\in\mathcal{C}^{(n)}$ (cf. (10)) are conditionally independent given the respective agent states $\boldsymbol{\theta}_i^{(n)}$ and $\boldsymbol{\theta}_j^{(n)}$. Thus we have

$$\begin{aligned}
&f\big(\mathbf{y}_{ij}^{(n)}\big|\boldsymbol{\theta}_i^{(n)},\boldsymbol{\theta}_j^{(n)}\big)\\
&= f\big(\mathbf{y}_{i\to j}^{(n)}\big|\boldsymbol{\theta}_i^{(n)},\boldsymbol{\theta}_j^{(n)}\big)\,f\big(\mathbf{y}_{j\to i}^{(n)}\big|\boldsymbol{\theta}_i^{(n)},\boldsymbol{\theta}_j^{(n)}\big)\\
&= \left(\prod_{k=1}^{K_{ij}} f\big(c_j\big(r_{ij}^{(n,k)}\big)\big|\boldsymbol{\theta}_i^{(n)},\boldsymbol{\theta}_j^{(n)}\big)\right)\prod_{k'=1}^{K_{ji}} f\big(c_i\big(r_{ji}^{(n,k')}\big)\big|\boldsymbol{\theta}_i^{(n)},\boldsymbol{\theta}_j^{(n)}\big)\\
&= G_{ij}^{(n)}\exp\left(-\frac{\|\mathbf{y}_{i\to j}^{(n)}-\boldsymbol{\psi}_{i\to j}^{(n)}\|^2}{2\alpha_j^{(n)2}\sigma_v^2}-\frac{\|\mathbf{y}_{j\to i}^{(n)}-\boldsymbol{\psi}_{j\to i}^{(n)}\|^2}{2\alpha_i^{(n)2}\sigma_v^2}\right), \quad (12)
\end{aligned}$$

where $G_{ij}^{(n)}\triangleq\big(\sqrt{2\pi}\,\alpha_j^{(n)}\sigma_v\big)^{-K_{ij}}\big(\sqrt{2\pi}\,\alpha_i^{(n)}\sigma_v\big)^{-K_{ji}}$, $\boldsymbol{\psi}_{i\to j}^{(n)}\triangleq\big[\psi_{i\to j}^{(n,1)}\big(\boldsymbol{\theta}_i^{(n)},\boldsymbol{\theta}_j^{(n)}\big)\cdots\psi_{i\to j}^{(n,K_{ij})}\big(\boldsymbol{\theta}_i^{(n)},\boldsymbol{\theta}_j^{(n)}\big)\big]^{\mathrm{T}}$, and $\boldsymbol{\psi}_{j\to i}^{(n)}\triangleq\big[\psi_{j\to i}^{(n,1)}\big(\boldsymbol{\theta}_i^{(n)},\boldsymbol{\theta}_j^{(n)}\big)\cdots\psi_{j\to i}^{(n,K_{ji})}\big(\boldsymbol{\theta}_i^{(n)},\boldsymbol{\theta}_j^{(n)}\big)\big]^{\mathrm{T}}$. As analyzed in [26], if the difference of successive packet transmit times is much larger than the noise standard deviation, i.e., $s_{ij}^{(n,k)}-s_{ij}^{(n,k-1)}\gg\sigma_v$ for $k=2,\ldots,K_{ij}$, then the following accurate approximation of the likelihood function (12) is obtained by approximating $\alpha_j^{(n)}\sigma_v$ and $\alpha_i^{(n)}\sigma_v$ (involved in $G_{ij}^{(n)}$) by σ_v:

$$\begin{aligned}
&f\big(\mathbf{y}_{ij}^{(n)}\big|\boldsymbol{\theta}_i^{(n)},\boldsymbol{\theta}_j^{(n)}\big)\\
&\quad\approx\tilde{f}\big(\mathbf{y}_{ij}^{(n)}\big|\boldsymbol{\theta}_i^{(n)},\boldsymbol{\theta}_j^{(n)}\big) \quad (13)\\
&\quad\propto\exp\left(-\frac{\big\|\mathbf{A}_{ij}^{(n)}\boldsymbol{\vartheta}_i^{(n)}+\mathbf{B}_{ij}^{(n)}\boldsymbol{\vartheta}_j^{(n)}+\mathbf{a}_d\|\mathbf{p}_i^{(n)}-\mathbf{p}_j^{(n)}\|\big\|^2}{2\sigma_v^2}\right), \quad (14)
\end{aligned}$$

where $\mathbf{A}_{ij}^{(n)}\triangleq\begin{bmatrix}\mathbf{1}_{K_{ij}} & -\tilde{\mathbf{y}}_{i\to j}^{(n)}\\ -\mathbf{1}_{K_{ji}} & \mathbf{y}_{j\to i}^{(n)}\end{bmatrix}$, $\mathbf{B}_{ij}^{(n)}\triangleq\begin{bmatrix}-\mathbf{1}_{K_{ij}} & \mathbf{y}_{i\to j}^{(n)}\\ \mathbf{1}_{K_{ji}} & -\tilde{\mathbf{y}}_{j\to i}^{(n)}\end{bmatrix}$, and $\mathbf{a}_d\triangleq-\frac{1}{c}\mathbf{1}_{K_{ij}+K_{ji}}$ with $\mathbf{1}_K$ denoting the all-ones vector of dimension K. In (14), $f\big(\mathbf{y}_{ij}^{(n)}\big|\boldsymbol{\theta}_i^{(n)},\boldsymbol{\theta}_j^{(n)}\big)$ is approximated by a Gaussian function in the agent distance $\|\mathbf{p}_i^{(n)}-\mathbf{p}_j^{(n)}\|$ and the clock states $\boldsymbol{\vartheta}_i^{(n)}$ and $\boldsymbol{\vartheta}_j^{(n)}$. As in [26], this approximation will allow us to develop a BP message passing scheme where the clock messages are represented by Gaussian parameters.

Finally, because $v_{ij}^{(n,k)}$ was assumed independent across n, we obtain the approximate joint likelihood function

$$\tilde{f}\big(\mathbf{y}^{(1:n)}\big|\boldsymbol{\theta}^{(1:n)}\big)=\prod_{n'=1}^{n}\prod_{\substack{(i,j)\in\mathcal{C}^{(n')}\\ i>j}}\tilde{f}\big(\mathbf{y}_{ij}^{(n')}\big|\boldsymbol{\theta}_i^{(n')},\boldsymbol{\theta}_j^{(n')}\big), \quad (15)$$

where $\mathbf{y}^{(1:n)}$ collects all $\mathbf{y}_{ij}^{(n')}$, $(i,j)\in\mathcal{C}^{(n')}$, $i>j$ and $\boldsymbol{\theta}^{(1:n)}$ collects all $\boldsymbol{\theta}_i^{(n')}$, $i\in\mathcal{I}$, both for $n'\in\{1,\ldots,n\}$.

IV. Sequential State Estimation Using BP

At each time step n, each agent $i\in\mathcal{I}$ estimates its current clock state $\boldsymbol{\vartheta}_i^{(n)}$ and location-related state $\mathbf{x}_i^{(n)}$ from all past and present measurements, $\mathbf{y}^{(1:n)}$. This is based on the minimum mean-square error (MMSE) estimates [33]

$$\hat{\boldsymbol{\vartheta}}_{i,\mathrm{MMSE}}^{(n)}\triangleq\int\boldsymbol{\vartheta}_i^{(n)}f\big(\boldsymbol{\vartheta}_i^{(n)}\big|\mathbf{y}^{(1:n)}\big)\,\mathrm{d}\boldsymbol{\vartheta}_i^{(n)}, \quad (16)$$

$$\hat{\mathbf{x}}_{i,\mathrm{MMSE}}^{(n)}\triangleq\int\mathbf{x}_i^{(n)}f\big(\mathbf{x}_i^{(n)}\big|\mathbf{y}^{(1:n)}\big)\,\mathrm{d}\mathbf{x}_i^{(n)}. \quad (17)$$

Here, the *marginal posterior pdfs* $f\big(\boldsymbol{\vartheta}_i^{(n)}\big|\mathbf{y}^{(1:n)}\big)$ and $f\big(\mathbf{x}_i^{(n)}\big|\mathbf{y}^{(1:n)}\big)$ can be obtained from the *joint posterior pdf* $f\big(\boldsymbol{\theta}^{(0:n)}\big|\mathbf{y}^{(1:n)}\big)\propto\tilde{f}\big(\mathbf{y}^{(1:n)}\big|\boldsymbol{\theta}^{(1:n)}\big)\,f\big(\boldsymbol{\theta}^{(0:n)}\big)$ by marginalizations. Because these marginalizations are typically computationally infeasible, we resort to approximate MMSE estimation by means of iterative BP [28]–[30]. BP provides approximations of the marginal posterior pdfs, $b\big(\boldsymbol{\vartheta}_i^{(n)}\big)\approx f\big(\boldsymbol{\vartheta}_i^{(n)}\big|\mathbf{y}^{(1:n)}\big)$ and $b\big(\mathbf{x}_i^{(n)}\big)\approx f\big(\mathbf{x}_i^{(n)}\big|\mathbf{y}^{(1:n)}\big)$, so-called *beliefs*, which can be calculated in a sequential (time-recursive), distributed manner. The means of these beliefs then provide approximations of the MMSE estimates $\hat{\boldsymbol{\vartheta}}_{i,\mathrm{MMSE}}^{(n)}$ and $\hat{\mathbf{x}}_{i,\mathrm{MMSE}}^{(n)}$.

A. Joint Posterior pdf and Factor Graph

BP is based on a factor graph (FG), which represents the factorization structure of the joint posterior pdf [28]–[30]. In our case, using the approximation (13) and the factorizations in (6) and (15), the joint posterior pdf is

$$\begin{aligned}
&f\big(\boldsymbol{\theta}^{(0:n)}\big|\mathbf{y}^{(1:n)}\big)\\
&\propto f\big(\boldsymbol{\theta}^{(0:n)}\big)\,\tilde{f}\big(\mathbf{y}^{(1:n)}\big|\boldsymbol{\theta}^{(1:n)}\big)\\
&=\prod_{i\in\mathcal{I}}f\big(\boldsymbol{\vartheta}_i^{(0)}\big)f\big(\mathbf{x}_i^{(0)}\big)\prod_{n'=1}^{n}f\big(\boldsymbol{\vartheta}_i^{(n')}\big|\boldsymbol{\vartheta}_i^{(n'-1)}\big)\,f\big(\mathbf{x}_i^{(n')}\big|\mathbf{x}_i^{(n'-1)}\big)\\
&\qquad\times\prod_{\substack{(i,j)\in\mathcal{C}^{(n')}\\ i>j}}\tilde{f}\big(\mathbf{y}_{ij}^{(n')}\big|\boldsymbol{\theta}_i^{(n')},\boldsymbol{\theta}_j^{(n')}\big). \quad (18)
\end{aligned}$$

In a direct application of BP, the maximum dimension of the messages would be the dimension of $\boldsymbol{\theta}_i^{(n)}$, i.e., six. To obtain

lower-dimensional messages, we apply the "opening nodes" principle [30, Sec. 5.2.2], i.e., we augment (18) by additional variables that depend deterministically on certain variables in (18). More specifically, we introduce location variable replicas $\tilde{\mathbf{p}}_i^{(n)} \triangleq \mathbf{P}\mathbf{x}_i^{(n)}$ (note that formally $\tilde{\mathbf{p}}_i^{(n)} = \mathbf{p}_i^{(n)}$) and interagent distances involving these location replicas, $d_{ij}^{(n)} \triangleq \big\|\tilde{\mathbf{p}}_i^{(n)} - \tilde{\mathbf{p}}_j^{(n)}\big\|$. In this way, the joint posterior pdf $f\big(\boldsymbol{\theta}^{(0:n)}\big|\mathbf{y}^{(1:n)}\big)$ in (18) is extended to

$$f\big(\boldsymbol{\theta}^{(0:n)}, \tilde{\mathbf{p}}^{(1:n)}, \mathbf{d}^{(1:n)}\big|\mathbf{y}^{(1:n)}\big) \propto f\big(\boldsymbol{\theta}^{(0:n)}, \tilde{\mathbf{p}}^{(1:n)}, \mathbf{d}^{(1:n)}\big) f\big(\mathbf{y}^{(1:n)}\big|\boldsymbol{\theta}^{(1:n)}, \tilde{\mathbf{p}}^{(1:n)}, \mathbf{d}^{(1:n)}\big), \quad (19)$$

where $\tilde{\mathbf{p}}^{(1:n)}$ consists of all $\tilde{\mathbf{p}}_i^{(n')}$ for $i \in \mathcal{I}$, and $\mathbf{d}^{(1:n)}$ consists of all $d_{ij}^{(n')}$ for $(i,j) \in \mathcal{C}^{(n')}$ $(i>j)$, both for $n' \in \{1,\dots,n\}$. The new likelihood function (cf. (15)) is

$$f\big(\mathbf{y}^{(1:n)}\big|\boldsymbol{\theta}^{(1:n)}, \tilde{\mathbf{p}}^{(1:n)}, \mathbf{d}^{(1:n)}\big) = \prod_{n'=1}^{n} \prod_{\substack{(i,j)\in\mathcal{C}^{(n')} \\ i>j}} \tilde{f}\big(\mathbf{y}_{ij}^{(n')}\big|\boldsymbol{\vartheta}_i^{(n')}, \boldsymbol{\vartheta}_j^{(n')}, d_{ij}^{(n')}\big), \quad (20)$$

where $\tilde{f}\big(\mathbf{y}_{ij}^{(n)}\big|\boldsymbol{\vartheta}_i^{(n)}, \boldsymbol{\vartheta}_j^{(n)}, d_{ij}^{(n)}\big)$ is given by (14) with $\big\|\mathbf{p}_i^{(n)} - \mathbf{p}_j^{(n)}\big\|$ replaced by $d_{ij}^{(n)}$. Here, we exploited the fact that the measurements $\mathbf{y}^{(1:n)}$ are conditionally independent of the location-related states given the interagent distances, i.e., $f\big(\mathbf{y}^{(1:n)}\big|\boldsymbol{\theta}^{(1:n)}, \tilde{\mathbf{p}}^{(1:n)}, \mathbf{d}^{(1:n)}\big) = f\big(\mathbf{y}^{(1:n)}\big|\boldsymbol{\vartheta}^{(1:n)}, \mathbf{d}^{(1:n)}\big)$. Furthermore, using (6) and the deterministic relations mentioned above, the extended prior pdf is obtained as

$$\begin{aligned} &f\big(\boldsymbol{\theta}^{(0:n)}, \tilde{\mathbf{p}}^{(1:n)}, \mathbf{d}^{(1:n)}\big) \\ &= f\big(\boldsymbol{\theta}^{(0:n)}\big) f\big(\tilde{\mathbf{p}}^{(1:n)}, \mathbf{d}^{(1:n)}\big|\boldsymbol{\theta}^{(0:n)}\big) \\ &= \prod_{i\in\mathcal{I}} f\big(\boldsymbol{\vartheta}_i^{(0)}\big) f\big(\mathbf{x}_i^{(0)}\big) \prod_{n'=1}^{n} f\big(\boldsymbol{\vartheta}_i^{(n')}\big|\boldsymbol{\vartheta}_i^{(n'-1)}\big) f\big(\mathbf{x}_i^{(n')}\big|\mathbf{x}_i^{(n'-1)}\big) \\ &\quad \times f\big(\tilde{\mathbf{p}}_i^{(n')}\big|\mathbf{x}_i^{(n')}\big) \prod_{\substack{(i,j)\in\mathcal{C}^{(n')} \\ i>j}} f\big(d_{ij}^{(n')}\big|\tilde{\mathbf{p}}_i^{(n')}, \tilde{\mathbf{p}}_j^{(n')}\big), \end{aligned} \quad (21)$$

where $f\big(d_{ij}^{(n)}\big|\tilde{\mathbf{p}}_i^{(n)}, \tilde{\mathbf{p}}_j^{(n)}\big) = \delta\big(d_{ij}^{(n)} - \big\|\tilde{\mathbf{p}}_i^{(n)} - \tilde{\mathbf{p}}_j^{(n)}\big\|\big)$ and $f\big(\tilde{\mathbf{p}}_i^{(n)}\big|\mathbf{x}_i^{(n)}\big) = \delta\big(\tilde{\mathbf{p}}_i^{(n)} - \mathbf{P}\mathbf{x}_i^{(n)}\big)$ express the deterministic relations $d_{ij}^{(n)} = \big\|\tilde{\mathbf{p}}_i^{(n)} - \tilde{\mathbf{p}}_j^{(n)}\big\|$ and $\tilde{\mathbf{p}}_i^{(n)} = \mathbf{P}\mathbf{x}_i^{(n)}$, respectively. Inserting (20) and (21) into (19), we obtain for the extended joint posterior pdf

$$\begin{aligned} &f\big(\boldsymbol{\theta}^{(0:n)}, \tilde{\mathbf{p}}^{(1:n)}, \mathbf{d}^{(1:n)}\big|\mathbf{y}^{(1:n)}\big) \\ &\propto \prod_{i\in\mathcal{I}} f\big(\boldsymbol{\vartheta}_i^{(0)}\big) f\big(\mathbf{x}_i^{(0)}\big) \prod_{n'=1}^{n} f\big(\boldsymbol{\vartheta}_i^{(n')}\big|\boldsymbol{\vartheta}_i^{(n'-1)}\big) f\big(\mathbf{x}_i^{(n')}\big|\mathbf{x}_i^{(n'-1)}\big) \\ &\quad \times f\big(\tilde{\mathbf{p}}_i^{(n')}\big|\mathbf{x}_i^{(n')}\big) \prod_{\substack{(i,j)\in\mathcal{C}^{(n')} \\ i>j}} \tilde{f}\big(\mathbf{y}_{ij}^{(n')}\big|\boldsymbol{\vartheta}_i^{(n')}, \boldsymbol{\vartheta}_j^{(n')}, d_{ij}^{(n')}\big) \\ &\quad \times f\big(d_{ij}^{(n')}\big|\tilde{\mathbf{p}}_i^{(n')}, \tilde{\mathbf{p}}_j^{(n')}\big). \end{aligned} \quad (22)$$

This extended joint posterior pdf is related to the original joint posterior pdf $f\big(\boldsymbol{\theta}^{(0:n)}\big|\mathbf{y}^{(1:n)}\big)$ (cf. (18)) via the marginalization $f(\boldsymbol{\theta}^{(0:n)}|\mathbf{y}^{(1:n)}) = \int\int f\big(\boldsymbol{\theta}^{(0:n)}, \tilde{\mathbf{p}}^{(1:n)}, \mathbf{d}^{(1:n)}\big|\mathbf{y}^{(1:n)}\big) \times \mathrm{d}\tilde{\mathbf{p}}^{(1:n)}\mathrm{d}\mathbf{d}^{(1:n)}$. In the factorization (22), all factors involve only state variables with a maximum dimension of four.

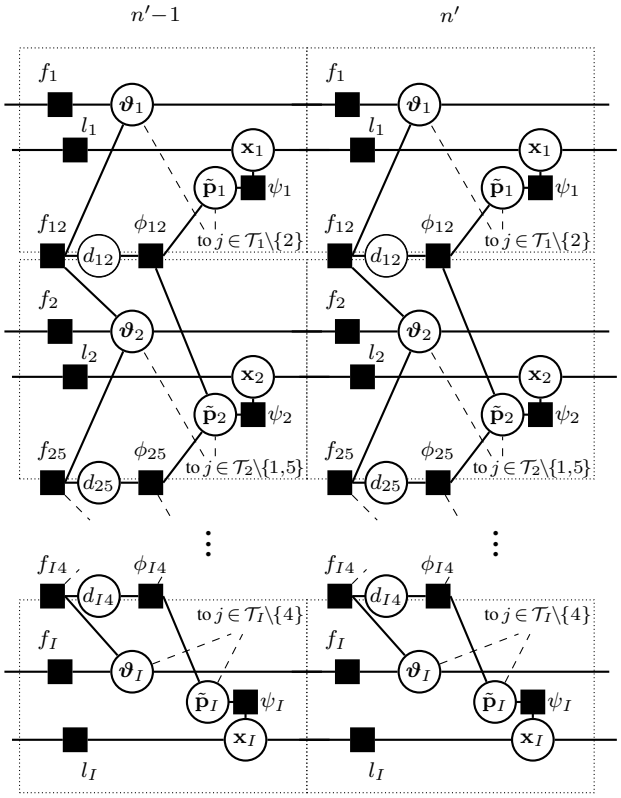

Fig. 3. CoSLAS factor graph for a network with agents $i \in \{1,2,\dots,I\}$, where $(1,2)$, $(2,5)$, and $(4,I)$ (and possibly other agent pairs) belong to both $\mathcal{C}^{(n'-1)}$ and $\mathcal{C}^{(n')}$. Only the time steps $n'-1$ and n' are shown. Time indices are omitted for simplicity (e.g., $\mathbf{x}_i$ is short for $\mathbf{x}_i^{(n'-1)}$ or $\mathbf{x}_i^{(n')}$). Each dotted box corresponds to an agent $i \in \mathcal{I}$ at time step $n'-1$ or n'; calculations within the box are performed locally by that agent. Connections between dotted boxes at the same time imply communication between agents.

The FG representing the factorization (22) is shown in Fig. 3. Each factor function in (22) is represented by a square factor node, and each variable by a circular variable node. A variable node is connected to a factor node by an edge if the corresponding variable is an argument of the corresponding factor function. In Fig. 3 and hereafter, we use the following short notations: $f_i \triangleq f\big(\boldsymbol{\vartheta}_i^{(n')}\big|\boldsymbol{\vartheta}_i^{(n'-1)}\big)$, $l_i \triangleq f\big(\mathbf{x}_i^{(n')}\big|\mathbf{x}_i^{(n'-1)}\big)$, $f_{ij} \triangleq \tilde{f}\big(\mathbf{y}_{ij}^{(n')}\big|\boldsymbol{\vartheta}_i^{(n')}, \boldsymbol{\vartheta}_j^{(n')}, d_{ij}^{(n')}\big)$, $\phi_{ij} \triangleq f\big(d_{ij}^{(n')}\big|\tilde{\mathbf{p}}_i^{(n')}, \tilde{\mathbf{p}}_j^{(n')}\big)$, and $\psi_i \triangleq f\big(\tilde{\mathbf{p}}_i^{(n')}\big|\mathbf{x}_i^{(n')}\big)$.

B. BP Message Passing

The proposed sequential CoSLAS algorithm applies BP [28], [29] to the FG in Fig. 3. Before presenting our algorithm in Section VI, we review the BP message update rules for a generic factor function f and a generic variable $\mathbf{z}$. Let $\mathcal{Z}_f$ denote the set of arguments of f, and assume $\mathbf{z} \in \mathcal{Z}_f$, i.e., $f = f(\mathbf{z}, \dots)$. Furthermore, let $\mathcal{F}_z$ denote the set of all functions f' of which $\mathbf{z}$ is an argument, i.e., $\mathbf{z} \in \mathcal{Z}_{f'}$ if and only if $f' \in \mathcal{F}_z$. The message from factor node f to variable node $\mathbf{z}$—denoted by $\zeta_f(\mathbf{z})$—and the message from variable node $\mathbf{z}$ to factor node f—denoted by $\eta_f(\mathbf{z})$—are calculated recursively as

$$\zeta_f(\mathbf{z}) = \int f(\mathbf{z},\ldots)\left(\prod_{\mathbf{z}'\in\mathcal{Z}_f\setminus\{\mathbf{z}\}} \eta_f(\mathbf{z}')\right) \mathrm{d}{\sim}\mathbf{z} \qquad (23)$$

and

$$\eta_f(\mathbf{z}) = \prod_{f'\in\mathcal{F}_z\setminus\{f\}} \zeta_{f'}(\mathbf{z})\,, \qquad (24)$$

where $\sim\mathbf{z}$ denotes all $\mathbf{z}'\in\mathcal{Z}_f$ except $\mathbf{z}$. Here we use the convention that an empty product (i.e., without any factors) is equal to one. After all messages have been calculated according to (23) and (24), the belief for variable $\mathbf{z}$ is obtained (up to a normalization) as

$$b(\mathbf{z}) \propto \prod_{f\in\mathcal{F}_z} \zeta_f(\mathbf{z})\,. \qquad (25)$$

For a function $f(\mathbf{z},\mathbf{z}')$ with only two arguments $\mathbf{z},\mathbf{z}'$, (23) simplifies to $\zeta_f(\mathbf{z}) = \int f(\mathbf{z},\mathbf{z}')\eta_f(\mathbf{z}')\mathrm{d}\mathbf{z}'$. If $\eta_f(\mathbf{z}')$ is a weighted S-component mixture distribution, then $\zeta_f(\mathbf{z})$ is again a weighted S-component mixture distribution, with the same weights.

If the FG is a tree, then the messages are calculated in a well-defined order (message schedule), starting with the leaf nodes, and the resulting beliefs are exactly equal to the respective marginal posterior pdfs [28], [29]. However, if the FG has loops, then the beliefs are only approximations of the marginal posterior pdfs. Moreover, the message calculations (23), (24) are repeated in an iterative manner, and convergence is not guaranteed for general non-Gaussian joint posterior pdfs. Finally, there exist many possible message schedules, which may lead to different beliefs, and the initialization of the messages is a degree of freedom. Nevertheless, loopy BP provides accurate approximations of the marginal posterior pdfs in many applications [21], [22], [26], [28]–[30].

As the CoSLAS FG in Fig. 3 contains loops, the sequential BP algorithm to be proposed in Section VI operates iteratively. The BP operations (23)–(25) follow a specific schedule that was observed to converge for the scenarios studied in Section VII. This schedule is chosen such that messages are not passed backward in time [22] and uninformative messages are censored [34] (i.e., not used in message calculations). Since the messages are not passed backward in time, our algorithm can cope with a changing network connectivity and its complexity does not increase with time n; moreover, the beliefs are directly equal to the messages passed to the next time. The algorithm consists of the following main steps:

1) *Prediction:* Each agent i locally converts the previous belief of its clock state, $b\big(\boldsymbol{\vartheta}_i^{(n-1)}\big)$, and of its location-related state, $b\big(\mathbf{x}_i^{(n-1)}\big)$, into messages $\zeta_{f_i}\big(\boldsymbol{\vartheta}_i^{(n)}\big)$ and $\zeta_{l_i}\big(\mathbf{x}_i^{(n)}\big)$ for the current time interval n. This corresponds to messages passed from the n'–1 section to the n' section along the horizontal edges of the FG in Fig. 3.
2) *Iterative message passing:* Each agent i exchanges messages related to its states $\boldsymbol{\vartheta}_i^{(n)}$ and $\tilde{\mathbf{p}}_i^{(n)}$ with neighboring agents, and uses the received messages to update its own messages according to (23) and (24). Only messages that are informative according to some criterion (see Section VI-B) are used for further calculations. In Fig. 3, these messages are passed along the edges connecting different agents in the same time interval, i.e., connecting sections that are aligned vertically. This step requires communication (packet exchanges) with neighboring agents; it is repeated during a predefined number of iterations Q.
3) *Belief calculation and estimation:* Each agent calculates its beliefs by multiplying according to (25) the appropriate messages calculated in Steps 1 and 2. It then uses these beliefs for state estimation according to (16) and (17), and as messages for the next prediction (Step 1).

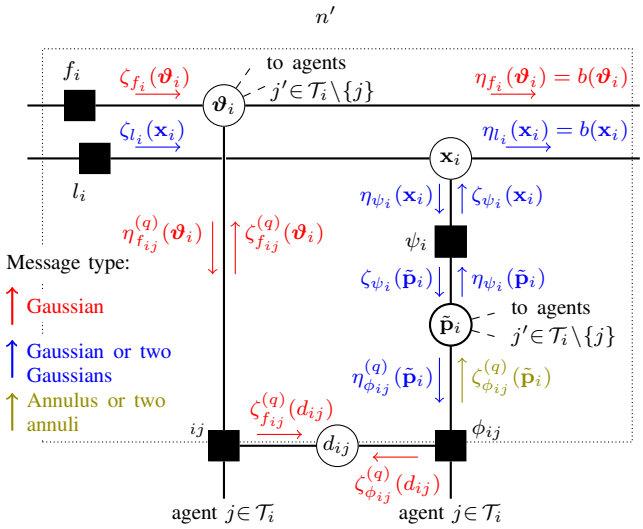

Fig. 4. Detail of the FG in Fig. 3, corresponding to agent i and its connection to agent $j\in\mathcal{T}_i$ at time step n'. All depicted messages are calculated by agent i. The messages $\eta_{f_{ij}}^{(q)}(d_{ij})$ and $\eta_{\phi_{ij}}^{(q)}(d_{ij})$, which are equal to $\zeta_{\phi_{ij}}^{(q)}(d_{ij})$ and $\zeta_{f_{ij}}^{(q)}(d_{ij})$, respectively, are omitted to avoid visual clutter. Messages represented by a single Gaussian are drawn in red, messages represented by a Gaussian or a two-component Gaussian mixture are drawn in blue, and messages represented by an annulus or two annuli are drawn in olive.

These steps will be worked out in Section VI after the introduction of parametric message representations.

V. Parametric Message Representations

The messages calculated at agent $i\in\mathcal{I}$ are displayed in the FG detail shown in Fig. 4. Hereafter, for simplicity, we drop the time index n in the superscript; furthermore the BP iteration index is denoted by the superscript $q\in\{1,\ldots,Q\}$. Note that in Fig. 4, each message is a function that represents a distribution of the function argument; e.g., $\eta_{f_{ij}}^{(q)}(\boldsymbol{\vartheta}_i)$ represents a distribution of the clock parameter $\boldsymbol{\vartheta}_i$. Furthermore, all messages with the iteration superscript $^{(q)}$ are computed during the *iterative message passing* step and are exchanged between neighbors (as specified below). All other messages are involved in the *prediction* and *belief calculation* steps and do not require any exchange with neighboring agents.

For the messages involved in the *prediction* and *belief calculation* steps, we use Gaussian or Gaussian mixture representations. More specifically, the clock messages $\zeta_{f_i}(\boldsymbol{\vartheta}_i)$ and $\eta_{f_i}(\boldsymbol{\vartheta}_i)$ are represented by a Gaussian, e.g., $\zeta_{f_i}(\boldsymbol{\vartheta}_i) = \mathcal{N}\big(\boldsymbol{\vartheta}_i;\boldsymbol{\mu}_{f_i\to\vartheta_i},\boldsymbol{\Sigma}_{f_i\to\vartheta_i}\big)$, and the location-related messages $\zeta_{l_i}(\mathbf{x}_i)$, $\eta_{l_i}(\mathbf{x}_i)$, $\zeta_{\psi_i}(\mathbf{x}_i)$, $\eta_{\psi_i}(\tilde{\mathbf{p}}_i)$, $\zeta_{\psi_i}(\tilde{\mathbf{p}}_i)$, and $\eta_{\psi_i}(\mathbf{x}_i)$ are

TABLE I
PARAMETERS OF THE MESSAGES INVOLVED IN THE PREDICTION AND BELIEF CALCULATION STEPS.

Message	$\boldsymbol{\mu}$	$\boldsymbol{\Sigma}$	w	$S \in \{1,2\}$
$\zeta_{f_i}(\boldsymbol{\vartheta}_i)$	$\boldsymbol{\mu}_{f_i \to \vartheta_i}$	$\boldsymbol{\Sigma}_{f_i \to \vartheta_i}$	—	—
$\zeta_{l_i}(\mathbf{x}_i) = \eta_{\psi_i}(\mathbf{x}_i)$	$\boldsymbol{\mu}_{l_i \to x_i,s}$	$\boldsymbol{\Sigma}_{l_i \to x_i,s}$	$w_{x_i,s}$	S_{x_i}
$\zeta_{\psi_i}(\tilde{\mathbf{p}}_i)$	$\boldsymbol{\mu}_{\psi_i \to \tilde{p}_i,s}$	$\boldsymbol{\Sigma}_{\psi_i \to \tilde{p}_i,s}$	$w_{x_i,s}$	S_{x_i}
$\eta_{\psi_i}(\tilde{\mathbf{p}}_i)$	$\boldsymbol{\mu}_{\tilde{p}_i \to \psi_i,s}$	$\boldsymbol{\Sigma}_{\tilde{p}_i \to \psi_i,s}$	$w_{\tilde{p}_i,s}$	$S_{\tilde{p}_i}$
$\zeta_{\psi_i}(\mathbf{x}_i)$	$\boldsymbol{\mu}_{\psi_i \to x_i,s}$	$\boldsymbol{\Sigma}_{\psi_i \to x_i,s}$	$w_{\tilde{p}_i,s}$	$S_{\tilde{p}_i}$
$\eta_{f_i}(\boldsymbol{\vartheta}_i) = b(\boldsymbol{\vartheta}_i)$	$\boldsymbol{\mu}_{\vartheta_i \to f_i}$	$\boldsymbol{\Sigma}_{\vartheta_i \to f_i}$	—	—
$\eta_{l_i}(\mathbf{x}_i) = b(\mathbf{x}_i)$	$\boldsymbol{\mu}_{x_i \to l_i,s}$	$\boldsymbol{\Sigma}_{x_i \to l_i,s}$	$w_{b_i,s}$	S_{b_i}

TABLE II
PARAMETERS OF THE MESSAGES INVOLVED IN THE ITERATIVE MESSAGE PASSING STEP.

Message	$\boldsymbol{\mu}$	$\boldsymbol{\Sigma}$	w	$S \in \{1,2\}$
$\eta_{f_{ij}}^{(q)}(\boldsymbol{\vartheta}_i)$	$\boldsymbol{\mu}_{\vartheta_i \to f_{ij}}^{(q)}$	$\boldsymbol{\Sigma}_{\vartheta_i \to f_{ij}}^{(q)}$	—	—
$\zeta_{f_{ij}}^{(q)}(\boldsymbol{\vartheta}_i)$	$\boldsymbol{\mu}_{f_{ij} \to \vartheta_i}^{(q)}$	$\boldsymbol{\Sigma}_{f_{ij} \to \vartheta_i}^{(q)}$	—	—
$\eta_{\phi_{ij}}^{(q)}(\tilde{\mathbf{p}}_i)$	$\boldsymbol{\mu}_{\tilde{p}_i \to \phi_{ij},s}^{(q)}$	$\boldsymbol{\Sigma}_{\tilde{p}_i \to \phi_{ij},s}^{(q)}$	$w_{i \to j,s}^{(q)}$	$S_{i \to j}^{(q)}$
$\eta_{\phi_{ij}}^{(q)}(d_{ij}) = \zeta_{f_{ij}}^{(q)}(d_{ij})$	$\mu_{f_{ij} \to d_{ij}}^{(q)}$	$\sigma_{f_{ij} \to d_{ij}}^{2\,(q)}$	—	—
$\eta_{f_{ij}}^{(q)}(d_{ij}) = \zeta_{\phi_{ij}}^{(q)}(d_{ij})$	$\mu_{\phi_{ij} \to d_{ij}}^{(q)}$	$\sigma_{\phi_{ij} \to d_{ij}}^{2\,(q)}$	—	—
$\zeta_{\phi_{ij}}^{(q)}(\tilde{\mathbf{p}}_i)$	$\boldsymbol{\mu}_{\phi_{ij},s}^{(q)}$	$\sigma_{\phi_{ij},s}^{2\,(q)}$	$w_{j \to i,s}^{(q-1)}$	$S_{j \to i}^{(q-1)}$

represented by a Gaussian or a two-component Gaussian mixture [23], [35], e.g.,

$$\zeta_{l_i}(\mathbf{x}_i) \triangleq \sum_{s=1}^{S_{x_i}} w_{x_i,s}\, \mathcal{N}\big(\mathbf{x}_i; \boldsymbol{\mu}_{l_i \to x_i,s}, \boldsymbol{\Sigma}_{l_i \to x_i,s}\big),$$

with $S_{x_i} \in \{1,2\}$ and normalized weights $w_{x_i,s}$. The latter representation is motivated by the observation that the location messages tend to be unimodal or bimodal [22]. Because l_i (short for $f\big(\mathbf{x}_i^{(n')}|\mathbf{x}_i^{(n'-1)}\big)$) has only two arguments, $\zeta_{l_i}(\mathbf{x}_i)$ has the same w and S parameters as $\eta_{l_i}(\mathbf{x}_i)$ from the previous time interval (cf. (23)). For the same reason, at function ψ_i (short for $f\big(\tilde{\mathbf{p}}_i|\mathbf{x}_i\big)$), $\eta_{\psi_i}(\mathbf{x}_i)$ and $\zeta_{\psi_i}(\tilde{\mathbf{p}}_i)$ have the same w and S parameters, and similarly for $\eta_{\psi_i}(\tilde{\mathbf{p}}_i)$ and $\zeta_{\psi_i}(\mathbf{x}_i)$. Moreover, since messages are not passed backward in time, we have $b(\boldsymbol{\vartheta}_i) = \eta_{f_i}(\boldsymbol{\vartheta}_i)$ (cf. (25) with only $\zeta_{f_i}(\boldsymbol{\vartheta}_i)\zeta_{f_{ij}}^{(Q)}(\boldsymbol{\vartheta}_i)$ on the right-hand side, which equals $\eta_{f_i}(\boldsymbol{\vartheta}_i)$ due to (24)) and similarly $b(\mathbf{x}_i) = \eta_{l_i}(\mathbf{x}_i)$, and $\eta_{\psi_i}(\mathbf{x}_i) = \zeta_{l_i}(\mathbf{x}_i)$ (cf. (24) with only $\zeta_{l_i}(\mathbf{x}_i)$ on the right-hand side). The notation used for the parameters of these messages is indicated in Table I.

Regarding the messages involved in the *iterative message passing* step, we use Gaussian representations for $\eta_{f_{ij}}^{(q)}(\boldsymbol{\vartheta}_i)$, $\zeta_{f_{ij}}^{(q)}(\boldsymbol{\vartheta}_i)$, $\zeta_{f_{ij}}^{(q)}(d_{ij})$, and $\zeta_{\phi_{ij}}^{(q)}(d_{ij})$, and Gaussian or two-component Gaussian mixture representations for $\eta_{\phi_{ij}}^{(q)}(\tilde{\mathbf{p}}_i)$ (here, $j \in \mathcal{T}_i$). The corresponding parameters are listed in Table II. For $\eta_{f_{ij}}^{(q)}(d_{ij})$ and $\eta_{\phi_{ij}}^{(q)}(d_{ij})$, the same Gaussian models as for, respectively, $\zeta_{\phi_{ij}}^{(q)}(d_{ij})$ and $\zeta_{f_{ij}}^{(q)}(d_{ij})$ are used, because $\eta_{f_{ij}}^{(q)}(d_{ij}) = \zeta_{\phi_{ij}}^{(q)}(d_{ij})$ and $\eta_{\phi_{ij}}^{(q)}(d_{ij}) = \zeta_{f_{ij}}^{(q)}(d_{ij})$ according to (24). Finally, $\zeta_{\phi_{ij}}^{(q)}(\tilde{\mathbf{p}}_i)$ is represented by an annulus or a mixture of two annuli defined as (cf. [35])

$$\zeta_{\phi_{ij}}^{(q)}(\tilde{\mathbf{p}}_i) \triangleq \sum_{s=1}^{S_{j \to i}^{(q-1)}} w_{j \to i,s}^{(q-1)} \exp\left(-\frac{\big(r_{\phi_{ij}}^{(q)} - \big\|\tilde{\mathbf{p}}_i - \boldsymbol{\mu}_{\phi_{ij},s}^{(q)}\big\|\big)^2}{2\sigma_{\phi_{ij},s}^{2\,(q)}}\right). \tag{26}$$

Here, $S_{j \to i}^{(q-1)}$ and $w_{j \to i,s}^{(q-1)}$ equal the S and w parameters of $\eta_{\phi_{ji}}^{(q-1)}(\tilde{\mathbf{p}}_j)$ (cf. Section VI-B4), $r_{\phi_{ij}}^{(q)}$ is the nominal radius of the annulus or annuli, and $\boldsymbol{\mu}_{\phi_{ij},s}^{(q)}$ and $\sigma_{\phi_{ij},s}^{2\,(q)}$ are, respectively, the center point and squared nominal width of annulus (mixture component) s. In each message passing iteration q, the parameters of these messages (see Table II) are calculated at agent i for all $j \in \mathcal{T}_i$, and the parameters of $\eta_{\phi_{ij}}^{(q)}(\tilde{\mathbf{p}}_i)$ and $\eta_{f_{ij}}^{(q)}(\boldsymbol{\vartheta}_i)$ are transmitted to neighbor agent j.

VI. THE PROPOSED COSLAS ALGORITHM

Although the BP algorithm reviewed in Section IV-B is less complex than straightforward marginalization of $f\big(\boldsymbol{\theta}^{(0:n)}\big|\mathbf{y}^{(1:n)}\big)$, a direct implementation of the BP rules (23)–(25) in the considered CoSLAS scenario is still computationally infeasible. Therefore, we next develop an approximate version of the BP algorithm that has moderate complexity and low communication requirements. This approximate algorithm is a hybrid particle-based and parametric implementation of (23)–(25): it combines a nonparametric (particle-based) BP implementation, which is typically used for the nonlinear cooperative localization problem [22], with parametric representations of messages and beliefs (see Section V), which are suited to the approximately linear-Gaussian synchronization problem [26]. This combination is enabled by the extended factorization (22) involving $\tilde{\mathbf{p}}_i$ and d_{ij}, whereby the location and clock states are characterized by separate messages and, thus, the message calculations can be performed via particle methods for the location states and via Gaussian parameter updates for the clock states. To obtain a distributed algorithm in which only message parameters have to be communicated between agents, the result of particle-based message multiplication for the location states is approximated by a Gaussian mixture (see Section V). Next, we present the individual operations used for calculating messages and beliefs.

A. Prediction

At time $n = 0$, the recursive BP algorithm is initialized by setting $b(\boldsymbol{\vartheta}_i) = f(\boldsymbol{\vartheta}_i)$ and $b(\mathbf{x}_i) = f(\mathbf{x}_i)$, where $f(\boldsymbol{\vartheta}_i)$ and $f(\mathbf{x}_i)$ are the Gaussian prior pdfs in (4) and (5). The mixture parameters of $\eta_{l_i}(\mathbf{x}_i) = b(\mathbf{x}_i) = f(\mathbf{x}_i)$ are $w_{b_i,1} = 1$ and $S_{b_i} = 1$. For $n \geq 1$, the parameters of the messages $\zeta_{f_i}(\boldsymbol{\vartheta}_i)$, $\zeta_{l_i}(\mathbf{x}_i)$, and $\zeta_{\psi_i}(\tilde{\mathbf{p}}_i)$ are calculated according to (23), in which the η messages are replaced by the respective beliefs b from time $n-1$ because they are equal. In the following presentation of these calculations, messages and their parameters that are used from time $n-1$ are denoted by the superscript "$-$". A

detailed derivation of the message parameter expressions in the subsequent equations (27)–(32) is provided in Appendix A.

1) Message $\zeta_{f_i}(\boldsymbol{\vartheta}_i)$: The parameters of $\zeta_{f_i}(\boldsymbol{\vartheta}_i)$ are calculated using the function f_i and the parameters of $b^-(\boldsymbol{\vartheta}_i)$. The evaluation of (23) here simplifies because the function node f_i is connected only to two edges [28]. One obtains

$$\boldsymbol{\mu}_{f_i\to\vartheta_i} = \boldsymbol{\mu}^-_{\vartheta_i\to f_i}\,, \tag{27}$$

$$\boldsymbol{\Sigma}_{f_i\to\vartheta_i} = \boldsymbol{\Sigma}^-_{\vartheta_i\to f_i} + \boldsymbol{\Sigma}_{u_{1,i}}\,. \tag{28}$$

2) Message $\zeta_{l_i}(\mathbf{x}_i)$: The parameters of $\zeta_{l_i}(\mathbf{x}_i)$ are calculated using the function l_i and the parameters of $b^-(\mathbf{x}_i)$. One obtains from (23)

$$\boldsymbol{\mu}_{l_i\to x_i,s} = \mathbf{G}_1\boldsymbol{\mu}^-_{x_i\to l_i,s}\,, \tag{29}$$

$$\boldsymbol{\Sigma}_{l_i\to x_i,s} = \mathbf{G}_1\boldsymbol{\Sigma}^-_{x_i\to l_i,s}\mathbf{G}_1^{\mathrm{T}} + \boldsymbol{\Sigma}_{u_{2,i}}\,, \tag{30}$$

as well as $w_{x_i,s}=w^-_{b_i,s}$ and $S_{x_i}=S^-_{b_i}$.

3) Message $\zeta_{\psi_i}(\tilde{\mathbf{p}}_i)$: Similarly, the parameters of $\zeta_{\psi_i}(\tilde{\mathbf{p}}_i)$ are calculated using the function ψ_i and the parameters of $\eta_{\psi_i}(\mathbf{x}_i)$. (Note that $\eta_{\psi_i}(\mathbf{x}_i)=\zeta_{l_i}(\mathbf{x}_i)$.) One obtains

$$\boldsymbol{\mu}_{\psi_i\to\tilde{p}_i,s} = \mathbf{P}\boldsymbol{\mu}_{l_i\to x_i,s}\,, \tag{31}$$

$$\boldsymbol{\Sigma}_{\psi_i\to\tilde{p}_i,s} = \mathbf{P}\boldsymbol{\Sigma}_{l_i\to x_i,s}\mathbf{P}^{\mathrm{T}}. \tag{32}$$

The w and S parameters are given by $w_{x_i,s}$ and S_{x_i}, respectively (see Section VI-A2).

B. Iterative Message Passing

Next, we describe the iterative message passing operations performed in iteration $q\in\{1,\dots,Q\}$. The iterations are initialized by setting $\eta^{(0)}_{f_{ij}}(\boldsymbol{\vartheta}_i)=\zeta_{f_i}(\boldsymbol{\vartheta}_i)$, $\eta^{(0)}_{\phi_{ij}}(\tilde{\mathbf{p}}_i)=\zeta_{\psi_i}(\tilde{\mathbf{p}}_i)$, and $\zeta^{(0)}_{f_{ij}}(d_{ij})=\zeta^{(0)}_{\phi_{ij}}(d_{ij})=f(d_{ij})$ for $j\in\mathcal{T}_i$, where $f(d_{ij})=\mathcal{N}(d_{ij};\mu_d,\sigma_d^2)$ with μ_d and σ_d^2 reflecting prior assumptions on the interagent distances. The messages $\eta^{(0)}_{f_{ij}}(\boldsymbol{\vartheta}_i)$ and $\eta^{(0)}_{\phi_{ij}}(\tilde{\mathbf{p}}_i)$ are passed to the neighbors $j\in\mathcal{T}_i$. For $q\geq 1$, the parameters of $\zeta^{(q)}_{f_{ij}}(d_{ij})$, $\zeta^{(q)}_{\phi_{ij}}(d_{ij})$, $\zeta^{(q)}_{f_{ij}}(\boldsymbol{\vartheta}_i)$, and $\zeta^{(q)}_{\phi_{ij}}(\tilde{\mathbf{p}}_i)$ are calculated according to (23), and the parameters of $\eta^{(q)}_{f_{ij}}(\boldsymbol{\vartheta}_i)$ and $\eta^{(q)}_{\phi_{ij}}(\tilde{\mathbf{p}}_i)$ are calculated according to (24), as discussed next.

1) Message $\zeta^{(q)}_{f_{ij}}(d_{ij})$: We consider message $\eta^{(q-1)}_{f_{ij}}(\boldsymbol{\vartheta}_i)$ (passed from agent i to neighbor j) as *informative* if $\big[\boldsymbol{\Sigma}^{(q-1)}_{\vartheta_i\to f_{ij}}\big]_{1,1}+\big[\boldsymbol{\Sigma}^{(q-1)}_{\vartheta_i\to f_{ij}}\big]_{2,2}T^2$ is smaller than a threshold τ, and we consider it as *uninformative* otherwise. Furthermore, we denote by $\mathcal{T}_i^{c(q)}$ the set of neighbors j of agent i that provide informative messages $\eta^{(q-1)}_{f_{ji}}(\boldsymbol{\vartheta}_j)$. If $\eta^{(q-1)}_{f_{ij}}(\boldsymbol{\vartheta}_i)$ is informative, then the parameters of $\zeta^{(q)}_{f_{ij}}(d_{ij})$, $j\in\mathcal{T}_i^{c(q)}$ are calculated using the function f_{ij} and the parameters of $\eta^{(q-1)}_{f_{ij}}(\boldsymbol{\vartheta}_i)$ and $\eta^{(q-1)}_{f_{ji}}(\boldsymbol{\vartheta}_j)$. Using (23) and standard Gaussian operations [28], one obtains (see Appendix A)

$$\sigma^{2\,(q)}_{f_{ij}\to d_{ij}} = \sigma_v^2\left(\|\mathbf{a}_d\|^2 - \mathbf{q}^{(q)\mathrm{T}}_{j\to i,1}\mathbf{D}_{ij}^{\mathrm{T}}\mathbf{a}_d\right)^{-1}, \tag{33}$$

$$\mu^{(q)}_{f_{ij}\to d_{ij}} = -\sigma^{2\,(q)}_{f_{ij}\to d_{ij}}\mathbf{q}^{(q)\mathrm{T}}_{j\to i,1}\,\boldsymbol{\Sigma}^{(q)\,-1}_{j\to i,1}\boldsymbol{\mu}^{(q)}_{j\to i,1}\,, \tag{34}$$

where $\mathbf{q}^{(q)\mathrm{T}}_{j\to i,1}\triangleq\mathbf{a}_d^{\mathrm{T}}\mathbf{D}_{ij}\big(\mathbf{D}_{ij}^{\mathrm{T}}\mathbf{D}_{ij}+\sigma_v^2\boldsymbol{\Sigma}^{(q)\,-1}_{j\to i,1}\big)^{-1}$, $\mathbf{D}_{ij}\triangleq[\mathbf{A}_{ij}\ \mathbf{B}_{ij}]$, $\boldsymbol{\Sigma}^{(q)}_{j\to i,1}\triangleq\mathrm{diag}\big\{\boldsymbol{\Sigma}^{(q-1)}_{\vartheta_i\to f_{ij}},\boldsymbol{\Sigma}^{(q-1)}_{\vartheta_j\to f_{ji}}\big\}$, and $\boldsymbol{\mu}^{(q)}_{j\to i,1}\triangleq\big[\boldsymbol{\mu}^{(q-1)\mathrm{T}}_{\vartheta_i\to f_{ij}}\ \boldsymbol{\mu}^{(q-1)\mathrm{T}}_{\vartheta_j\to f_{ji}}\big]^{\mathrm{T}}$. Otherwise, i.e., if $\eta^{(q-1)}_{f_{ij}}(\boldsymbol{\vartheta}_i)$ is uninformative or if $j\notin\mathcal{T}_i^{c(q)}$, we set $\zeta^{(q)}_{f_{ij}}(d_{ij})=\zeta^{(q-1)}_{f_{ij}}(d_{ij})$.

2) Message $\zeta^{(q)}_{\phi_{ij}}(d_{ij})$: We consider $\eta^{(q-1)}_{\phi_{ij}}(\tilde{\mathbf{p}}_i)$ as informative if it satisfies a criterion involving two thresholds τ_1 and τ_2 (see Section VI-B6), and we denote by $\mathcal{T}_i^{p(q)}$ the set of neighbors j of agent i that provide informative messages $\eta^{(q-1)}_{\phi_{ji}}(\tilde{\mathbf{p}}_j)$. If $\eta^{(q-1)}_{\phi_{ij}}(\tilde{\mathbf{p}}_i)$ is informative, then the parameters of $\zeta^{(q)}_{\phi_{ij}}(d_{ij})$, $j\in\mathcal{T}_i^{p(q)}$ are calculated using the function ϕ_{ij} and the parameters of $\eta^{(q-1)}_{\phi_{ij}}(\tilde{\mathbf{p}}_i)$ and $\eta^{(q-1)}_{\phi_{ji}}(\tilde{\mathbf{p}}_j)$. Because ϕ_{ij} is nonlinear, we use a linearization as discussed in Appendix B. This yields a single Gaussian representing $\zeta^{(q)}_{\phi_{ij}}(d_{ij})$, whose mean and variance are obtained as

$$\mu^{(q)}_{\phi_{ij}\to d_{ij}} = \sum_{r=1}^{S^{(q-1)}_{i\to j}}\sum_{s=1}^{S^{(q-1)}_{j\to i}} w^{(q-1)}_{i\to j,r}\,w^{(q-1)}_{j\to i,s}\,\big\|\boldsymbol{\mu}^{(q-1)}_{d_{ij},rs}\big\|\,, \tag{35}$$

$$\sigma^{2\,(q)}_{\phi_{ij}\to d_{ij}} = \sum_{r=1}^{S^{(q-1)}_{i\to j}}\sum_{s=1}^{S^{(q-1)}_{j\to i}} w^{(q-1)}_{i\to j,r}\,w^{(q-1)}_{j\to i,s}\Big(\bar{\boldsymbol{\mu}}^{(q-1)\mathrm{T}}_{d_{ij},rs}\boldsymbol{\Sigma}_{ij,rs}\bar{\boldsymbol{\mu}}^{(q-1)}_{d_{ij},rs} + \big(\big\|\boldsymbol{\mu}^{(q-1)}_{d_{ij},rs}\big\| - \mu^{(q)}_{\phi_{ij}\to d_{ij}}\big)^2\Big), \tag{36}$$

with $\boldsymbol{\mu}^{(q-1)}_{d_{ij},rs}\triangleq\boldsymbol{\mu}^{(q-1)}_{\tilde{p}_i\to\phi_{ij},r}-\boldsymbol{\mu}^{(q-1)}_{\tilde{p}_j\to\phi_{ji},s}$, $\boldsymbol{\Sigma}_{ij,rs}\triangleq\mathrm{diag}\big\{\boldsymbol{\Sigma}^{(q-1)}_{\tilde{p}_i\to\phi_{ij},r},\boldsymbol{\Sigma}^{(q-1)}_{\tilde{p}_j\to\phi_{ji},s}\big\}$, and $\bar{\boldsymbol{\mu}}^{(q-1)}_{d_{ij},rs}\triangleq\big[\boldsymbol{\mu}^{(q-1)\mathrm{T}}_{d_{ij},rs}\ -\boldsymbol{\mu}^{(q-1)\mathrm{T}}_{d_{ij},rs}\big]^{\mathrm{T}}/\big\|\boldsymbol{\mu}^{(q-1)}_{d_{ij},rs}\big\|$. If $\eta^{(q-1)}_{\phi_{ij}}(\tilde{\mathbf{p}}_i)$ is uninformative or if $j\notin\mathcal{T}_i^{p(q)}$, we set $\zeta^{(q)}_{\phi_{ij}}(d_{ij})=\zeta^{(q-1)}_{\phi_{ij}}(d_{ij})$.

3) Message $\zeta^{(q)}_{f_{ij}}(\boldsymbol{\vartheta}_i)$: The parameters of $\zeta^{(q)}_{f_{ij}}(\boldsymbol{\vartheta}_i)$, $j\in\mathcal{T}_i^{c(q)}$ are calculated using the function f_{ij} and the parameters of $\eta^{(q-1)}_{f_{ji}}(\boldsymbol{\vartheta}_j)$ and $\eta^{(q)}_{f_{ij}}(d_{ij})=\zeta^{(q)}_{\phi_{ij}}(d_{ij})$. Similarly to (33) and (34), one has (see Appendix A)

$$\boldsymbol{\Sigma}^{(q)}_{f_{ij}\to\vartheta_i} = \sigma_v^2\left(\mathbf{A}_{ij}^{\mathrm{T}}\mathbf{A}_{ij} - \mathbf{Q}^{(q)}_{j\to i,2}\mathbf{C}_{ij}^{\mathrm{T}}\mathbf{A}_{ij}\right)^{-1}, \tag{37}$$

$$\boldsymbol{\mu}^{(q)}_{f_{ij}\to\vartheta_i} = -\boldsymbol{\Sigma}^{(q)}_{f_{ij}\to\vartheta_i}\mathbf{Q}^{(q)}_{j\to i,2}\boldsymbol{\Sigma}^{(q)\,-1}_{j\to i,2}\,\boldsymbol{\mu}^{(q)}_{j\to i,2}\,, \tag{38}$$

where $\mathbf{Q}^{(q)}_{j\to i,2}\triangleq\mathbf{A}_{ij}^{\mathrm{T}}\mathbf{C}_{ij}\big(\mathbf{C}_{ij}^{\mathrm{T}}\mathbf{C}_{ij}+\sigma_v^2\boldsymbol{\Sigma}^{(q)\,-1}_{j\to i,2}\big)^{-1}$, $\mathbf{C}_{ij}\triangleq[\mathbf{B}_{ij}\ \mathbf{a}_d]$, $\boldsymbol{\Sigma}^{(q)}_{j\to i,2}\triangleq\mathrm{diag}\big\{\boldsymbol{\Sigma}^{(q-1)}_{\vartheta_j\to f_{ji}},\sigma^{2\,(q-1)}_{\phi_{ij}\to d_{ij}}\big\}$, and $\boldsymbol{\mu}^{(q)}_{j\to i,2}\triangleq\big[\boldsymbol{\mu}^{(q-1)\mathrm{T}}_{\vartheta_j\to f_{ji}}\ \mu^{(q-1)}_{\phi_{ij}\to d_{ij}}\big]^{\mathrm{T}}$.

4) Message $\zeta^{(q)}_{\phi_{ij}}(\tilde{\mathbf{p}}_i)$: The parameters of $\zeta^{(q)}_{\phi_{ij}}(\tilde{\mathbf{p}}_i)$, $j\in\mathcal{T}_i^{p(q)}$ (see (26)) are calculated using the function ϕ_{ij} and the parameters of $\eta^{(q-1)}_{\phi_{ji}}(\tilde{\mathbf{p}}_j)$ and $\eta^{(q)}_{\phi_{ij}}(d_{ij})=\zeta^{(q)}_{f_{ij}}(d_{ij})$. Again, because ϕ_{ij} is nonlinear, we linearize $\|\tilde{\mathbf{p}}_i-\tilde{\mathbf{p}}_j\|$ (considered as a function of $\tilde{\mathbf{p}}_i$, with fixed $\tilde{\mathbf{p}}_j=\boldsymbol{\mu}^{(q-1)}_{\tilde{p}_j\to\phi_{ji},s}$, $s\in\{1,\dots,S^{(q-1)}_{j\to i}\}$) around $\sum_{r=1}^{S^{(q-1)}_{i\to j}}w^{(q-1)}_{i\to j,r}\boldsymbol{\mu}^{(q-1)}_{\tilde{p}_i\to\phi_{ij},r}$ and obtain the parameters of (26) as [31], [35]

$$r^{(q)}_{\phi_{ij}} = \mu^{(q)}_{f_{ij}\to d_{ij}}\,,$$

$$\boldsymbol{\mu}^{(q)}_{\phi_{ij},s} = \boldsymbol{\mu}^{(q-1)}_{\tilde{p}_j\to\phi_{ji},s}\,,$$

$$\sigma^{2\,(q)}_{\phi_{ij},s} = \bar{\boldsymbol{\mu}}^{(q-1)\mathrm{T}}_{p_{ij},s}\,\boldsymbol{\Sigma}^{(q-1)}_{\tilde{p}_j\to\phi_{ji},s}\,\bar{\boldsymbol{\mu}}^{(q-1)}_{p_{ij},s} + \sigma^{2\,(q)}_{f_{ij}\to d_{ij}}\,,$$

where $\bar{\boldsymbol{\mu}}^{(q-1)}_{p_{ij},s}\triangleq\boldsymbol{\mu}^{(q-1)}_{p_{ij},s}/\big\|\boldsymbol{\mu}^{(q-1)}_{p_{ij},s}\big\|$ with $\boldsymbol{\mu}^{(q-1)}_{p_{ij},s}\triangleq\boldsymbol{\mu}^{(q-1)}_{\tilde{p}_j\to\phi_{ji},s}-\sum_{r=1}^{S^{(q-1)}_{i\to j}}w^{(q-1)}_{i\to j,r}\boldsymbol{\mu}^{(q-1)}_{\tilde{p}_i\to\phi_{ij},r}$. Furthermore, $w^{(q-1)}_{j\to i,s}$ and $S^{(q-1)}_{j\to i}$

in (26) equal the respective parameters of $\eta_{\phi_{ji}}^{(q-1)}(\tilde{\mathbf{p}}_j)$ (cf. Section VI-B6). In this context, note that $\zeta_{\phi_{ij}}^{(q)}(\tilde{\mathbf{p}}_i) = \iint f(d_{ij}|\tilde{\mathbf{p}}_i, \tilde{\mathbf{p}}_j)\, \eta_{\phi_{ji}}^{(q-1)}(\tilde{\mathbf{p}}_j)\, \eta_{\phi_{ij}}^{(q)}(d_{ij})\, \mathrm{d}\tilde{\mathbf{p}}_j\, \mathrm{d}d_{ij}$ (cf. (23)) involves only $\eta_{\phi_{ji}}^{(q-1)}(\tilde{\mathbf{p}}_j)$ as Gaussian mixture distribution whereas $\eta_{\phi_{ij}}^{(q)}(d_{ij})$ is a Gaussian distribution.

5) Message $\eta_{f_{ij}}^{(q)}(\boldsymbol{\vartheta}_i)$: The parameters of $\eta_{f_{ij}}^{(q)}(\boldsymbol{\vartheta}_i)$, $j \in \mathcal{T}_i$ are calculated from those of $\zeta_{f_i}(\boldsymbol{\vartheta}_i)$ and $\zeta_{f_{ij'}}^{(q)}(\boldsymbol{\vartheta}_i)$, $j' \in \mathcal{T}_i^{c(q)} \setminus \{j\}$ according to (24). Since all involved messages are Gaussian, $\eta_{f_{ij}}^{(q)}(\boldsymbol{\vartheta}_i)$ is a single Gaussian with parameters [28]

$$\boldsymbol{\Sigma}_{\vartheta_i \to f_{ij}}^{(q)} = \left(\boldsymbol{\Sigma}_{f_i \to \vartheta_i}^{-1} + \sum_{j' \in \mathcal{T}_i^{c(q)} \setminus \{j\}} \boldsymbol{\Sigma}_{f_{ij'} \to \vartheta_i}^{(q)\,-1} \right)^{-1}, \tag{39}$$

$$\boldsymbol{\mu}_{\vartheta_i \to f_{ij}}^{(q)} = \boldsymbol{\Sigma}_{\vartheta_i \to f_{ij}}^{(q)} \Bigg(\boldsymbol{\Sigma}_{f_i \to \vartheta_i}^{-1} \boldsymbol{\mu}_{f_i \to \vartheta_i} + \sum_{j' \in \mathcal{T}_i^{c(q)} \setminus \{j\}} \boldsymbol{\Sigma}_{f_{ij'} \to \vartheta_i}^{(q)\,-1} \boldsymbol{\mu}_{f_{ij'} \to \vartheta_i}^{(q)} \Bigg). \tag{40}$$

6) Message $\eta_{\phi_{ij}}^{(q)}(\tilde{\mathbf{p}}_i)$: The parameters of $\eta_{\phi_{ij}}^{(q)}(\tilde{\mathbf{p}}_i)$, $j \in \mathcal{T}_i$ are calculated from those of $\zeta_{\psi_i}(\tilde{\mathbf{p}}_i)$ and $\zeta_{\phi_{ij'}}^{(q)}(\tilde{\mathbf{p}}_i)$, $j' \in \mathcal{T}_i^{p(q)} \setminus \{j\}$ via (24), which reads

$$\eta_{\phi_{ij}}^{(q)}(\tilde{\mathbf{p}}_i) = \zeta_{\psi_i}(\tilde{\mathbf{p}}_i) \prod_{j' \in \mathcal{T}_i^{p(q)} \setminus \{j\}} \zeta_{\phi_{ij'}}^{(q)}(\tilde{\mathbf{p}}_i). \tag{41}$$

This product involves the annularly shaped messages $\zeta_{\phi_{ij'}}^{(q)}(\tilde{\mathbf{p}}_i)$ (see (26)). We use a particle implementation of (41) based on importance sampling [36], which is inspired by an approach proposed for localization in [21] and [35]. The resulting particle representation of $\eta_{\phi_{ij}}^{(q)}(\tilde{\mathbf{p}}_i)$ is then approximated by a Gaussian or Gaussian mixture distribution, or the message $\eta_{\phi_{ij}}^{(q)}(\tilde{\mathbf{p}}_i)$ is declared uninformative as explained presently.

The proposal distribution for importance sampling is chosen similarly as in [21], i.e.,

$$p^{(q)}(\tilde{\mathbf{p}}_i) \triangleq \zeta_{\psi_i}(\tilde{\mathbf{p}}_i) + \sum_{j' \in \mathcal{T}_i^{p(q)} \setminus \{j\}} \zeta_{\phi_{ij'}}^{(q)}(\tilde{\mathbf{p}}_i). \tag{42}$$

To obtain particles representing $p^{(q)}(\tilde{\mathbf{p}}_i)$, we first draw particles $\{\tilde{\mathbf{p}}_{\zeta_i,i}^{(l)}\}_{l=1}^{L}$ from the Gaussian or Gaussian mixture message $\zeta_{\psi_i}(\tilde{\mathbf{p}}_i)$. Next, for each $j' \in \mathcal{T}_i^{p(q)} \setminus \{j\}$, we generate particles $\{\tilde{\mathbf{p}}_{\zeta_{ij'},i}^{(l)}\}_{l=1}^{L}$ representing $\zeta_{\phi_{ij'}}^{(q)}(\tilde{\mathbf{p}}_i)$ according to [21]

$$\tilde{\mathbf{p}}_{\zeta_{ij'},i}^{(l)} = \tilde{\mathbf{p}}_{\eta_{ij'},j'}^{(l)} + d_{ij'}^{(l)} \begin{bmatrix} \sin(\varphi^{(l)}) \\ \cos(\varphi^{(l)}) \end{bmatrix}.$$

This involves particles $\{\tilde{\mathbf{p}}_{\eta_{ij'},j'}^{(l)}\}_{l=1}^{L}$ drawn from $\eta_{\phi_{ij'}}^{(q-1)}(\tilde{\mathbf{p}}_{j'})$, particles $\{d_{ij'}^{(l)}\}_{l=1}^{L}$ drawn from $\eta_{f_{ij'}}^{(q)}(d_{ij'})$, and particles $\{\varphi^{(l)}\}_{l=1}^{L}$ drawn uniformly on $[0, 2\pi)$. Then, $|\mathcal{T}_i^{p(q)}|L$ particles $\{\tilde{\mathbf{p}}_i^{(l)}\}_{l=1}^{|\mathcal{T}_i^{p(q)}|L}$ representing the proposal distribution $p^{(q)}(\tilde{\mathbf{p}}_i)$ in (42) are obtained by fusing the particles $\{\tilde{\mathbf{p}}_{\zeta_i,i}^{(l)}\}_{l=1}^{L}$ and $\{\tilde{\mathbf{p}}_{\zeta_{ij'},i}^{(l)}\}_{l=1}^{L}$, $j' \in \mathcal{T}_i^{p(q)} \setminus \{j\}$, i.e.,

$$\{\tilde{\mathbf{p}}_i^{(l)}\}_{l=1}^{|\mathcal{T}_i^{p(q)}|L} = \{\tilde{\mathbf{p}}_{\zeta_i,i}^{(l)}\}_{l=1}^{L} \cup \bigcup_{j' \in \mathcal{T}_i^{p(q)} \setminus \{j\}} \{\tilde{\mathbf{p}}_{\zeta_{ij'},i}^{(l)}\}_{l=1}^{L}.$$

The corresponding weights are calculated as

$$w_i^{(l)} = \frac{\eta_{\phi_{ij}}^{(q)}(\tilde{\mathbf{p}}_i^{(l)})}{p^{(q)}(\tilde{\mathbf{p}}_i^{(l)})} = \frac{\zeta_{\psi_i}(\tilde{\mathbf{p}}_i^{(l)}) \prod_{j' \in \mathcal{T}_i^{p(q)} \setminus \{j\}} \zeta_{\phi_{ij'}}^{(q)}(\tilde{\mathbf{p}}_i^{(l)})}{\zeta_{\psi_i}(\tilde{\mathbf{p}}_i^{(l)}) + \sum_{j' \in \mathcal{T}_i^{p(q)} \setminus \{j\}} \zeta_{\phi_{ij'}}^{(q)}(\tilde{\mathbf{p}}_i^{(l)})},$$

for $l = 1, \ldots, |\mathcal{T}_i^{p(q)}|L$. This involves an evaluation of the messages $\zeta_{\psi_i}(\tilde{\mathbf{p}}_i)$ (cf. Section VI-A3) and $\zeta_{\phi_{ij'}}^{(q)}(\tilde{\mathbf{p}}_i)$, $j' \in \mathcal{T}_i^{p(q)} \setminus \{j\}$ in (26) at the particles $\tilde{\mathbf{p}}_i^{(l)}$, $l = 1, \ldots, |\mathcal{T}_i^{p(q)}|L$. The complexity of this algorithm for computing the message product (41) scales only linearly in the number of particles. This improves on the quadratic scaling of the particle-based message multiplication method described in [21].

Next, following [35], the weighted particle representation $\{(\tilde{\mathbf{p}}_i^{(l)}, w_i^{(l)})\}_{l=1}^{|\mathcal{T}_i^{p(q)}|L}$ of $\eta_{\phi_{ij}}^{(q)}(\tilde{\mathbf{p}}_i)$ is converted into a Gaussian or two-component Gaussian mixture distribution, or the respective message is declared uninformative. We first use a clustering algorithm such as k-means++ [37] to split the weighted particle set $\{(\tilde{\mathbf{p}}_i^{(l)}, w_i^{(l)})\}_{l=1}^{|\mathcal{T}_i^{p(q)}|L}$ into two disjoint subsets $\{(\tilde{\mathbf{p}}_i^{(l)}, w_i^{(l)})\}_{l \in \mathcal{L}_s}$, $s \in \{1, 2\}$, where $\mathcal{L}_s$ is the subset of particle indices for cluster s. For each cluster $s \in \{1, 2\}$, we calculate a mean vector $\boldsymbol{\mu}_{\tilde{p}_i \to \phi_{ij},s}^{(q)}$ and a covariance matrix $\boldsymbol{\Sigma}_{\tilde{p}_i \to \phi_{ij},s}^{(q)}$ as, respectively, the weighted sample mean and weighted sample covariance of $\{(\tilde{\mathbf{p}}_i^{(l)}, w_i^{(l)})\}_{l \in \mathcal{L}_s}$. If the two particle subsets $\{(\tilde{\mathbf{p}}_i^{(l)}, w_i^{(l)})\}_{l \in \mathcal{L}_1}$ and $\{(\tilde{\mathbf{p}}_i^{(l)}, w_i^{(l)})\}_{l \in \mathcal{L}_2}$ do not "overlap" too much, in the sense that their Fisher discriminant [37] is larger than a threshold τ_1, and if their means are sufficiently far apart in the sense that $\|\boldsymbol{\mu}_{\tilde{p}_i \to \phi_{ij},1}^{(q)} - \boldsymbol{\mu}_{\tilde{p}_i \to \phi_{ij},2}^{(q)}\|$ is larger than a threshold τ_2, then we approximate $\eta_{\phi_{ij}}^{(q)}(\tilde{\mathbf{p}}_i)$ by a two-component Gaussian mixture distribution, i.e., we set $S_{i \to j}^{(q)} = 2$. The mean and covariance of Gaussian component $s \in \{1, 2\}$ are then given by $\boldsymbol{\mu}_{\tilde{p}_i \to \phi_{ij},s}^{(q)}$ and $\boldsymbol{\Sigma}_{\tilde{p}_i \to \phi_{ij},s}^{(q)}$, respectively, and the weight is given by $w_{i \to j,s}^{(q)} = \tilde{w}_{i \to j,s}^{(q)} / W_i$ with $\tilde{w}_{i \to j,s}^{(q)} = \sum_{l \in \mathcal{L}_s} w_i^{(l)}$ and $W_i = \tilde{w}_{i \to j,1}^{(q)} + \tilde{w}_{i \to j,2}^{(q)}$.

Otherwise, i.e., if at least one of the above-mentioned threshold criteria is violated, we calculate the weighted sample mean and weighted sample covariance of the entire particle set, which are denoted by $\boldsymbol{\mu}_{\tilde{p}_i \to \phi_{ij},1}^{(q)}$ and $\boldsymbol{\Sigma}_{\tilde{p}_i \to \phi_{ij},1}^{(q)}$, respectively. (Note that this notation conforms to the indexing convention defined by Table II.) If the trace of $\boldsymbol{\Sigma}_{\tilde{p}_i \to \phi_{ij},1}^{(q)}$ is smaller than a threshold τ_3, we approximate $\eta_{\phi_{ij}}^{(q)}(\tilde{\mathbf{p}}_i)$ by a single Gaussian distribution ($S_{i \to j}^{(q)} = 1$ and $w_{i \to j,1}^{(q)} = 1$) with mean $\boldsymbol{\mu}_{\tilde{p}_i \to \phi_{ij},1}^{(q)}$ and covariance $\boldsymbol{\Sigma}_{\tilde{p}_i \to \phi_{ij},1}^{(q)}$. Otherwise, the message $\eta_{\phi_{ij}}^{(q)}(\tilde{\mathbf{p}}_i)$ is declared to be uninformative. The threshold parameter τ_1 is chosen heuristically. The parameters τ_2 and $\sqrt{\tau_3}$ are related to the uncertainty of the distances, and are set roughly an order of magnitude larger than the presumed uncertainty of the distance estimates (evaluated as $\sigma_v c/K$, with the noise standard deviation σ_v, the speed of light c, and the average number of packets K). Our simulations showed that the

proposed method is not very sensitive to the precise choice of the threshold parameters.

C. Calculation of Messages $\eta_{\psi_i}(\tilde{\mathbf{p}}_i)$ and $\zeta_{\psi_i}(\mathbf{x}_i)$

The messages $\eta_{\psi_i}(\tilde{\mathbf{p}}_i)$ and $\zeta_{\psi_i}(\mathbf{x}_i)$ are calculated after the final message passing iteration ($q = Q$).

1) Message $\eta_{\psi_i}(\tilde{\mathbf{p}}_i)$: According to (24),

$$\eta_{\psi_i}(\tilde{\mathbf{p}}_i) = \prod_{j \in \mathcal{T}_i^{p(Q)}} \zeta_{\phi_{ij}}^{(Q)}(\tilde{\mathbf{p}}_i)\,.$$

If $\mathcal{T}_i^{p(Q)}$ is nonempty, then a Gaussian or Gaussian mixture distribution with parameters $\boldsymbol{\mu}_{\tilde{p}_i \to \psi_i, s}$, $\boldsymbol{\Sigma}_{\tilde{p}_i \to \psi_i, s}$, $w_{\tilde{p}_i, s}$, and $S_{\tilde{p}_i} \in \{1, 2\}$ is obtained by carrying out similar steps as in Section VI-B6, using the proposal distribution $p(\tilde{\mathbf{p}}_i) \triangleq \sum_{j \in \mathcal{T}_i^{p(Q)}} \zeta_{\phi_{ij}}^{(Q)}(\tilde{\mathbf{p}}_i)$ and replacing $S_{i \to j}^{(q)}$ by $S_{\tilde{p}_i}$. If $\mathcal{T}_i^{p(Q)}$ is empty or if $\eta_{\psi_i}(\tilde{\mathbf{p}}_i)$ is found to be uninformative, then $\eta_{\psi_i}(\tilde{\mathbf{p}}_i)$ is set to a constant (i.e., $\boldsymbol{\Sigma}^{-1}_{\tilde{p}_i \to \psi_i, s}$ is set to the zero matrix).

2) Message $\zeta_{\psi_i}(\mathbf{x}_i)$: The parameters of $\zeta_{\psi_i}(\mathbf{x}_i)$ are calculated from those of $\eta_{\psi_i}(\tilde{\mathbf{p}}_i)$ based on (23). One obtains

$$\begin{aligned} \boldsymbol{\Sigma}^{-1}_{\psi_i \to x_i, s} &= \mathbf{P}^{\mathrm{T}} \boldsymbol{\Sigma}^{-1}_{\tilde{p}_i \to \psi_i, s} \mathbf{P}\,, \\ \boldsymbol{\Sigma}^{-1}_{\psi_i \to x_i, s} \boldsymbol{\mu}_{\psi_i \to x_i, s} &= \mathbf{P}^{\mathrm{T}} \boldsymbol{\Sigma}^{-1}_{\tilde{p}_i \to \psi_i, s} \boldsymbol{\mu}_{\tilde{p}_i \to \psi_i, s}\,. \end{aligned} \tag{43}$$

Note that (43) yields $\boldsymbol{\Sigma}^{-1}_{\psi_i \to x_i, s} \boldsymbol{\mu}_{\psi_i \to x_i, s}$ (instead of $\boldsymbol{\mu}_{\psi_i \to x_i, s}$) because that product will be used in (45). The w and S parameters are $w_{\tilde{p}_i, s}$ and $S_{\tilde{p}_i}$ (see Section VI-C1).

D. Calculation of Beliefs

Once the parameters of $\eta_{\psi_i}(\tilde{\mathbf{p}}_i)$ and $\zeta_{\psi_i}(\mathbf{x}_i)$ are available, the beliefs $b(\boldsymbol{\vartheta}_i)$ and $b(\mathbf{x}_i)$ are calculated according to (25).

1) Belief $b(\boldsymbol{\vartheta}_i)$: The parameters $\boldsymbol{\Sigma}_{\vartheta_i \to f_i}$ and $\boldsymbol{\mu}_{\vartheta_i \to f_i}$ of belief $b(\boldsymbol{\vartheta}_i) = \eta_{f_i}(\boldsymbol{\vartheta}_i)$ are calculated from those of $\zeta_{f_i}(\boldsymbol{\vartheta}_i)$ and $\zeta_{f_{ij}}^{(Q)}(\boldsymbol{\vartheta}_i)$, $j \in \mathcal{T}_i^{c(Q)}$. This is done by calculating the expressions in (39) and (40), respectively, in which q is replaced by Q, the summation index set $\mathcal{T}_i^{c(q)} \setminus \{j\}$ is replaced by $\mathcal{T}_i^{c(Q)}$, and all the terms involving $\boldsymbol{\Sigma}^{-1}_{f_i \to \vartheta_i}$ are suppressed.

2) Belief $b(\mathbf{x}_i)$: The parameters $\boldsymbol{\mu}_{x_i \to l_i, s}$, $\boldsymbol{\Sigma}_{x_i \to l_i, s}$, $w_{b_i, s}$, and $S_{b_i} \in \{1, 2\}$ of belief $b(\mathbf{x}_i) = \eta_{l_i}(\mathbf{x}_i)$ are obtained by multiplying $\zeta_{\psi_i}(\mathbf{x}_i)$ and $\zeta_{l_i}(\mathbf{x}_i)$. These messages are mixtures of, respectively, $S_{\tilde{p}_i}$ and S_{x_i} components. This results in $S_{\tilde{p}_i} S_{x_i}$ mixture components for $b(\mathbf{x}_i)$, with parameters

$$\boldsymbol{\Sigma}_{x_i \to l_i, (r,s)} = \big(\boldsymbol{\Sigma}^{-1}_{\psi_i \to x_i, r} + \boldsymbol{\Sigma}^{-1}_{l_i \to x_i, s}\big)^{-1}, \tag{44}$$

$$\begin{aligned} \boldsymbol{\mu}_{x_i \to l_i, (r,s)} = \boldsymbol{\Sigma}_{x_i \to l_i, (r,s)} \big(&\boldsymbol{\Sigma}^{-1}_{\psi_i \to x_i, r} \boldsymbol{\mu}_{\psi_i \to x_i, r} \\ &+ \boldsymbol{\Sigma}^{-1}_{l_i \to x_i, s} \boldsymbol{\mu}_{l_i \to x_i, s}\big) \end{aligned} \tag{45}$$

and weights (before normalization)

$$\begin{aligned} \tilde{w}_{b_i, (r,s)} = w_{\tilde{p}_i, r} w_{x_i, s} \\ \times \exp\big(-h_{\psi_i \to x_i, r} - h_{l_i \to x_i, s} + h_{x_i \to l_i, (r,s)}\big)\,, \end{aligned}$$

where $h_{\psi_i \to x_i, r} \triangleq \boldsymbol{\mu}^{\mathrm{T}}_{\psi_i \to x_i, r} \boldsymbol{\Sigma}^{-1}_{\psi_i \to x_i, r} \boldsymbol{\mu}_{\psi_i \to x_i, r}$, $h_{l_i \to x_i, s} \triangleq \boldsymbol{\mu}^{\mathrm{T}}_{l_i \to x_i, s} \boldsymbol{\Sigma}^{-1}_{l_i \to x_i, s} \boldsymbol{\mu}_{l_i \to x_i, s}$, and $h_{x_i \to l_i, (r,s)} \triangleq \boldsymbol{\mu}^{\mathrm{T}}_{x_i \to l_i, (r,s)} \times \boldsymbol{\Sigma}^{-1}_{x_i \to l_i, (r,s)} \boldsymbol{\mu}_{x_i \to l_i, (r,s)}$. Note that $S_{\tilde{p}_i} S_{x_i}$ may be 1, 2, or 4. If $S_{\tilde{p}_i} S_{x_i}$ is 1 or 2, we use all the mixture components to represent the product message $b(\mathbf{x}_i)$, i.e., $S_{b_i} = S_{\tilde{p}_i} S_{x_i}$, and the final weights $w_{b_i, (r,s)}$ are obtained by normalizing the $\tilde{w}_{b_i, (r,s)}$. However, if $S_{\tilde{p}_i} S_{x_i} = 4$, we set $S_{b_i} = 2$ and use only the two strongest mixture components, corresponding to the two index tuples (r, s) whose weights $\tilde{w}_{b_i, (r,s)}$ are largest. These weights are then normalized. The parameters and weights obtained in this way are then assigned to $\boldsymbol{\Sigma}_{x_i \to l_i, s'}$, $\boldsymbol{\mu}_{x_i \to l_i, s'}$, and $w_{b_i, s'}$ with $s' \in \{1, \ldots, S_{b_i}\}$.

E. Estimation

Approximations $\hat{\boldsymbol{\vartheta}}_i^{(n)}$ and $\hat{\mathbf{x}}_i^{(n)}$ of the MMSE estimates $\hat{\boldsymbol{\vartheta}}_{i,\mathrm{MMSE}}^{(n)}$ and $\hat{\mathbf{x}}_{i,\mathrm{MMSE}}^{(n)}$ are obtained by replacing in (16) and (17) the marginal posterior pdfs $f\big(\boldsymbol{\vartheta}_i^{(n)} \big| \mathbf{y}^{(1:n)}\big)$ and $f\big(\mathbf{x}_i^{(n)} \big| \mathbf{y}^{(1:n)}\big)$ by the beliefs $b(\boldsymbol{\vartheta}_i)$ and $b(\mathbf{x}_i)$, respectively. Using the parametric representations of $b(\boldsymbol{\vartheta}_i)$ and $b(\mathbf{x}_i)$ discussed in Sections V and VI-D, $\hat{\boldsymbol{\vartheta}}_i^{(n)}$ is directly given by $\boldsymbol{\mu}_{\vartheta_i \to f_i}$, and $\hat{\mathbf{x}}_i^{(n)}$ by $\sum_{s \in S_{b_i}} w_{b_i, s} \boldsymbol{\mu}_{x_i \to l_i, s}$. Finally, estimates of the primary clock parameters $\alpha_i^{(n)}$ and $\beta_i^{(n)}$ (see Section II-A) are obtained as $\hat{\alpha}_i^{(n)} = 1/[\hat{\boldsymbol{\vartheta}}_i^{(n)}]_2$ and $\hat{\beta}_i^{(n)} = \hat{\alpha}_i^{(n)} [\hat{\boldsymbol{\vartheta}}_i^{(n)}]_1$.

F. Algorithm Summary and Communication Requirements

A summary of the overall algorithm is provided in Table III. Note that the algorithm is distributed since all agents execute their operations in parallel, there is no fusion center, and interagent communication is limited to neighboring agents. Since the algorithm operates iteratively, its convergence behavior is of importance. Convergence of loopy BP can be proved for Gaussian models [38], as in the case of pure synchronization [26]. However, it cannot be guaranteed for general models, which are relevant to localization and, hence, SLAS. A common way to study the convergence behavior of loopy BP is by numerical simulation [22]. In our simulation of the proposed BP algorithm, we always observed convergence.

The communication requirements per agent, message passing iteration, and neighbor are as follows. At any time n, in any message passing iteration q, the parameters of the two-dimensional messages $\eta_{\phi_{ij}}^{(q)}(\tilde{\mathbf{p}}_i)$ and $\eta_{f_{ij}}^{(q)}(\boldsymbol{\vartheta}_i)$ have to be transmitted from agent i to agent $j \in \mathcal{T}_i^{(n)}$. According to Section VI-B6, $\eta_{\phi_{ij}}^{(q)}(\tilde{\mathbf{p}}_i)$ is either uninformative or represented by a Gaussian or two-component Gaussian mixture distribution. In the last case, which corresponds to maximum communication requirements, the parameters of $\eta_{\phi_{ij}}^{(q)}(\tilde{\mathbf{p}}_i)$ are two mean vectors, two covariance matrices, and one weight (as the two weights are normalized, only one of them has to be known). Furthermore, according to Section VI-B5, $\eta_{f_{ij}}^{(q)}(\boldsymbol{\vartheta}_i)$ is represented by a single Gaussian, i.e., by one mean vector and one covariance matrix. Hence, the total number of real values that have to be transmitted from agent $i \in \mathcal{I}$ to agent $j \in \mathcal{T}_i^{(n)}$ per iteration q is maximally $(2 \cdot 2 + 2 \cdot 3 + 1) + (2 + 3) = 16$.

VII. Numerical Study

In this section, we analyze the performance of the proposed CoSLAS algorithm and compare it with that of two variants with perfect clock or location-velocity information.

TABLE III
COSLAS BP ALGORITHM—OPERATIONS PERFORMED BY AGENT i

Initialization at time $n=0$:

The temporal recursion is initialized by setting $b(\boldsymbol{\vartheta}_i) = f\big(\boldsymbol{\vartheta}_i^{(0)}\big)$ and $b(\mathbf{x}_i) = f\big(\mathbf{x}_i^{(0)}\big)$ (see (4) and (5), respectively).

Temporal recursion at times $n \geq 1$:

Step 1 – Prediction:

1.1) The clock message $\zeta_{f_i}(\boldsymbol{\vartheta}_i)$ is calculated from $b^-(\boldsymbol{\vartheta}_i)$ (which was calculated at time $n-1$) according to (27) and (28).

1.2) The location message $\zeta_{l_i}(\mathbf{x}_i)$ is calculated from $b^-(\mathbf{x}_i)$ (which was calculated at time $n-1$) according to Section VI-A2.

1.3) The location message $\zeta_{\psi_i}(\tilde{\mathbf{p}}_i)$ is calculated from $\eta_{\psi_i}(\mathbf{x}_i) = \zeta_{l_i}(\mathbf{x}_i)$ according to Section VI-A3.

Step 2 – Iterative message passing: The message passing iteration is initialized by setting $\eta_{f_{ij}}^{(0)}(\boldsymbol{\vartheta}_i) = \zeta_{f_i}(\boldsymbol{\vartheta}_i)$, $\eta_{\phi_{ij}}^{(0)}(\tilde{\mathbf{p}}_i) = \zeta_{\psi_i}(\tilde{\mathbf{p}}_i)$, and $\zeta_{f_{ij}}^{(0)}(d_{ij}) = \zeta_{\phi_{ij}}^{(0)}(d_{ij}) = f(d_{ij})$ for all $j \in \mathcal{T}_i$. Furthermore, $\eta_{f_{ij}}^{(0)}(\boldsymbol{\vartheta}_i)$ and $\eta_{\phi_{ij}}^{(0)}(\tilde{\mathbf{p}}_i)$ are transmitted to the respective neighbors $j \in \mathcal{T}_i$. Then, for $q = 1, \ldots, Q$:

2.1) The messages $\eta_{f_{ji}}^{(q-1)}(\boldsymbol{\vartheta}_j)$ and $\eta_{\phi_{ji}}^{(q-1)}(\tilde{\mathbf{p}}_j)$ (calculated at the previous iteration) are received from the respective neighbors $j \in \mathcal{T}_i$. The sets $\mathcal{T}_i^{c(q)} = \big\{j \big| \eta_{f_{ji}}^{(q-1)}(\boldsymbol{\vartheta}_j) \text{ is informative}\big\}$ and $\mathcal{T}_i^{p(q)} = \big\{j \big| \eta_{\phi_{ji}}^{(q-1)}(\tilde{\mathbf{p}}_j) \text{ is informative}\big\}$ are determined.

2.2) If $\eta_{f_{ij}}^{(q-1)}(\boldsymbol{\vartheta}_i)$ is informative, then for all $j \in \mathcal{T}_i^{c(q)}$, the messages $\zeta_{f_{ij}}^{(q)}(d_{ij})$ are calculated from $\eta_{f_{ij}}^{(q-1)}(\boldsymbol{\vartheta}_i)$ and $\eta_{f_{ji}}^{(q-1)}(\boldsymbol{\vartheta}_j)$ according to (33) and (34). Otherwise $\zeta_{f_{ij}}^{(q)}(d_{ij}) = \zeta_{f_{ij}}^{(q-1)}(d_{ij})$.

2.3) If $\eta_{\phi_{ij}}^{(q-1)}(\tilde{\mathbf{p}}_i)$ is informative, then for all $j \in \mathcal{T}_i^{p(q)}$, the messages $\zeta_{\phi_{ij}}^{(q)}(d_{ij})$ are calculated from $\eta_{\phi_{ij}}^{(q-1)}(\tilde{\mathbf{p}}_i)$ and $\eta_{\phi_{ji}}^{(q-1)}(\tilde{\mathbf{p}}_j)$ according to to (35) and (36). Otherwise $\zeta_{\phi_{ij}}^{(q)}(d_{ij}) = \zeta_{\phi_{ij}}^{(q-1)}(d_{ij})$.

2.4) For $j \in \mathcal{T}_i^{c(q)}$, the messages $\zeta_{f_{ij}}^{(q)}(\boldsymbol{\vartheta}_i)$ are calculated from $\eta_{f_{ji}}^{(q-1)}(\boldsymbol{\vartheta}_j)$ and $\zeta_{\phi_{ij}}^{(q)}(d_{ij})$ according to (37) and (38).

2.5) For $j \in \mathcal{T}_i^{p(q)}$, the messages $\zeta_{\phi_{ij}}^{(q)}(\tilde{\mathbf{p}}_i)$ are calculated from $\eta_{\phi_{ji}}^{(q-1)}(\tilde{\mathbf{p}}_j)$ and $\zeta_{f_{ij}}^{(q)}(d_{ij})$ according to Section VI-B4.

2.6) For $j \in \mathcal{T}_i$, the messages $\eta_{f_{ij}}^{(q)}(\boldsymbol{\vartheta}_i)$ are calculated from $\zeta_{f_i}(\boldsymbol{\vartheta}_i)$ and $\zeta_{f_{ij'}}^{(q)}(\boldsymbol{\vartheta}_i)$, $j' \in \mathcal{T}_i^{c(q)} \setminus \{j\}$ according to (39) and (40).

2.7) For $j \in \mathcal{T}_i$, the messages $\eta_{\phi_{ij}}^{(q)}(\tilde{\mathbf{p}}_i)$ are calculated from $\zeta_{\psi_i}(\tilde{\mathbf{p}}_i)$ and $\zeta_{\phi_{ij'}}^{(q)}(\tilde{\mathbf{p}}_i)$, $j' \in \mathcal{T}_i^{p(q)} \setminus \{j\}$ according to Section VI-B6.

2.8) The (parameters of) the messages $\eta_{f_{ij}}^{(q)}(\boldsymbol{\vartheta}_i)$ and $\eta_{\phi_{ij}}^{(q)}(\tilde{\mathbf{p}}_i)$ are transmitted to the respective neighbors $j \in \mathcal{T}_i$.

Step 3 – Belief calculation:

3.1) The belief $b(\boldsymbol{\vartheta}_i)$ is calculated from $\zeta_{f_i}(\boldsymbol{\vartheta}_i)$ and $\zeta_{f_{ij}}^{(Q)}(\boldsymbol{\vartheta}_i)$, $j \in \mathcal{T}_i^{c(Q)}$ according to (39) and (40) in which q is replaced by Q, the summation index set $\mathcal{T}_i^{c(q)} \setminus \{j\}$ is replaced by $\mathcal{T}_i^{c(Q)}$, and all terms involving $\boldsymbol{\Sigma}_{f_i \to \vartheta_i}^{-1}$ are suppressed.

3.2) The message $\eta_{\psi_i}(\tilde{\mathbf{p}}_i)$ is calculated from $\zeta_{\phi_{ij}}^{(Q)}(\tilde{\mathbf{p}}_i)$, $j \in \mathcal{T}_i^{p(Q)}$ according to Section VI-C1. Next, the message $\zeta_{\psi_i}(\mathbf{x}_i)$ is calculated from $\eta_{\psi_i}(\tilde{\mathbf{p}}_i)$ according to Section VI-C2. Finally, the belief $b(\mathbf{x}_i)$ is calculated from $\zeta_{\psi_i}(\mathbf{x}_i)$ and $\zeta_{l_i}(\mathbf{x}_i)$ according to Section VI-D2.

Step 4 – Estimation: The clock estimates $\hat{\alpha}_i$ and $\hat{\beta}_i$ and the location-related estimates $\hat{\mathbf{x}}_i$ are obtained from the parameters of $b(\boldsymbol{\vartheta}_i)$ and $b(\mathbf{x}_i)$, respectively as described in Section VI-E.

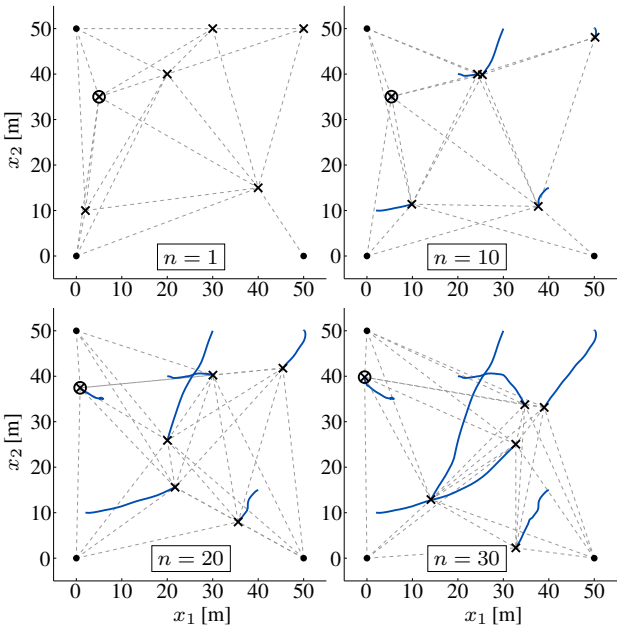

Fig. 5. Agent locations at times $n = 1$, 10, 20, and 30. Dots indicate the locations of the spatial reference agents, crosses indicate the locations of the mobile agents, the circle indicates the location of the temporal reference agent (one of the mobile agents), blue solid lines indicate the agent trajectories, and dashed gray lines indicate the measurement/communication links.

A. Simulation Setting

We consider a network of $I = 9$ agents located in a square area of size $50\,\mathrm{m} \times 50\,\mathrm{m}$, as shown in Fig. 5. The time interval length is $T = 1\,\mathrm{s}$. Three of the agents ($i \in \{1, 2, 3\}$) are nonmobile[1] spatial references located in three corners of the square area, and the remaining six agents ($i \in \{4, \ldots, 9\}$) are mobile. Mobile agent $i = 7$ is a clock reference with known fixed clock state $\boldsymbol{\vartheta}_7^{(n)} = [0\ \ 1]^{\mathrm{T}}$ for all n. For $i \neq 7$, the clock states $\boldsymbol{\vartheta}_i^{(n)}$ evolve according to (2) with process noise standard deviations $\sigma_{1,i} = 1\,\mu\mathrm{s}$ and $\sigma_{2,i} = 10\,\mathrm{ppm}$, and with the initial clock states $\boldsymbol{\vartheta}_i^{(0)}$, $i \neq 7$ randomly drawn according to (4) with $\sigma_{\nu_i} = 1\,\mathrm{s}$, $\sigma_{\lambda_i} = 150\,\mathrm{ppm}$, and $\boldsymbol{\mu}_{f_{i \to \vartheta_i}}^{(0)} = [0\ \ 1]^{\mathrm{T}}$. The location-related states $\mathbf{x}_i^{(n)}$ of the mobile agents evolve according to (3) with process noise standard deviation $\sigma_{u_2,i} = 2\,\mathrm{m}$, and with the initial values $\mathbf{x}_i^{(0)}$ chosen as shown in Fig. 5. A realization of the states $\boldsymbol{\vartheta}_i^{(n)}$ and $\mathbf{x}_i^{(n)}$, $n = 0, 1, \ldots$ was generated as described above and used for all simulation runs. Fig. 5 shows the locations of the agents at four different times n.

Each agent communicates with other agents within a radius of $40\,\mathrm{m}$, i.e., $\mathcal{T}_i^{(n)} = \big\{j \in \mathcal{I} \setminus \{i\} \big| \big\|\mathbf{p}_i^{(n)} - \mathbf{p}_j^{(n)}\big\| \leq 40\,\mathrm{m}\big\}$. The network connectivity is time-varying (cf. Fig. 5) but the network is always connected, as assumed in Section II-A. The agents perform $K_{ij} = K_{ji} = 10$ noisy measurements relative to each neighbor according to (7). In each of the 100 simulation runs we performed, the measurement noises $v_{ij}^{(n,k)}$ in (7) were drawn independently for all $(i, j) \in \mathcal{C}^{(n)}$, n, and $k \in \{1, \ldots, K_{ij} = 10\}$, with a noise standard deviation of $\sigma_v = 10\,\mathrm{ns}$.

In the simulated algorithms, the parameters used to initialize the distance messages $\zeta_{f_{ij}}^{(0)}(d_{ij}) = \zeta_{\phi_{ij}}^{(0)}(d_{ij})$ (see Section

[1]The extension to mobile spatial reference nodes is straightforward.

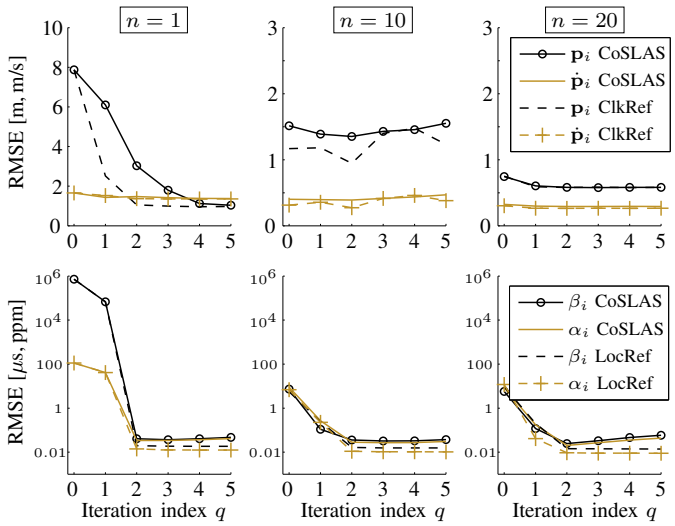

Fig. 6. RMSEs versus message passing iteration index q at times $n = 1$, 10, and 20. Top: location-related parameters, bottom: clock parameters.

VI-B) are $\mu_d = 27\,\mathrm{m}$ and $\sigma_d = 10\,\mathrm{m}$. The process noise parameters and the parameters σ_{ν_i} and σ_{λ_i} are as stated earlier. The number of particles used for message multiplication (see Section VI-B6) is $\left|\mathcal{T}_i^{p(q)}\right| L = 1000$ unless noted otherwise. The threshold parameters (see Section VI-B) are $\tau = 2\,\mathrm{s}^2$, $\tau_1 = 15$, $\tau_2 = 5\,\mathrm{m}$, and $\tau_3 = 40\,\mathrm{m}^2$. The initial covariance matrix of $\mathbf{x}_i^{(0)}$, $\mathbf{\Sigma}_{l_i \to x_i}^{(0)}$ (see (5)), is defined by $\sigma_{x_i} = 5\,\mathrm{m}$ and $\sigma_{\dot{x}_i} = 2\,\mathrm{m/s}$, and the initial mean is modeled randomly as $\boldsymbol{\mu}_{l_i \to x_i}^{(0)} = \mathbf{x}_i^{(0)} + \boldsymbol{\varepsilon}_i$, where $\mathbf{x}_i^{(0)}$ is the actual initial location-related state and $\boldsymbol{\varepsilon}_i \sim \mathcal{N}\big(\boldsymbol{\varepsilon}_i; \mathbf{0}, \mathbf{\Sigma}_{l_i \to x_i}^{(0)}\big)$ is drawn independently for all i and all simulation runs.

B. Simulation Results

We consider the proposed CoSLAS algorithm (briefly referred to as CoSLAS) and two variants performing only localization or synchronization. In the first variant, dubbed ClkRef, all agents know their clock parameters, and in the second variant, LocRef, all agents know their location and velocity. We are not able to present a comparison with other methods because, to the best of our knowledge, there are no other SLAS methods for time-varying clock skew and clock offset. Our measure of performance is the root mean square error (RMSE) of the various parameters using averaging over 100 simulation runs and over those agents that are not reference agents.

For times $n = 1$, 10, and 20, Fig. 6 shows the dependence of the RMSEs of location, velocity, clock phase, and clock skew (cf. Section VI-E) on the message passing iteration index q. Here, differently from Section VI-E and Table III, the belief calculation and estimation steps were performed in each iteration q, for a total of $Q = 5$ iterations. At $n = 1$, the RMSE of the locations $\mathbf{p}_i$ is seen to converge to a minimum after $q = 4$ iterations for CoSLAS and after $q = 2$ iterations for ClkRef. This difference can be explained by the fact that in ClkRef, all agents know their clocks whereas in CoSLAS, distance messages can only be calculated when the agents possess informative clock messages (cf. Step 2.2 in Table III). Furthermore, the RMSE of $\dot{\mathbf{p}}_i$ does not decrease with increasing q. This can be explained as follows. Via (44) and (45), the location accuracy expressed by $\zeta_{\psi_i}(\mathbf{x}_i)$ and $\zeta_{l_i}(\mathbf{x}_i)$—or, more specifically, by the first two (block) entries of the corresponding parameters $\boldsymbol{\mu}_{\psi_i \to x_i, r}$, $\mathbf{\Sigma}_{\psi_i \to x_i, r}$ and $\boldsymbol{\mu}_{l_i \to x_i, s}$, $\mathbf{\Sigma}_{l_i \to x_i, s}$, respectively—strongly influences the velocity accuracy expressed by $b(\mathbf{x}_i)$—or, more specifically, by the second two (block) entries of $\boldsymbol{\mu}_{x_i \to l_i, s}$, $\mathbf{\Sigma}_{x_i \to l_i, s}$. But at $n = 1$, $\zeta_{l_i}(\mathbf{x}_i)$ still contains large uncertainties inherited from the initial prior $f\big(\mathbf{x}_i^{(0)}\big)$. Therefore, $\dot{\mathbf{p}}_i$ cannot be estimated accurately at time $n = 1$. The RMSEs of the clock parameters α_i and β_i converge to a minimum after $q = 2$ iterations for both CoSLAS and LocRef. We note that $q = 2$ iterations correspond to the maximum hop distance from any nonreference agent to a spatial/temporal reference agent (in each iteration, the clock and location information is propagated by one hop).[2]

At $n = 10$ and $n = 20$, the RMSEs of α_i and β_i converge to a minimum in $q = 2$ iterations. At $n = 10$, the RMSE of $\mathbf{p}_i$ is rather high for all q. This is because the top right agent in the "$n = 10$" part of Fig. 5 has two of its three neighbors effectively located in the same direction. This is no longer the case at $n = 20$, and indeed the RMSE of $\mathbf{p}_i$ here converges approximately to a minimum in only $q = 1$ iteration. Thus, one can obtain low communication cost without compromising the convergence of $\mathbf{p}_i$ by performing only one message passing iteration per time step ($Q = 1$, which is sometimes referred to as "real-time BP" [39]). We also see that at $n = 10$ and $n = 20$, remarkably, the RMSEs of CoSLAS are similar to or only slightly higher than those of ClkRef and LocRef. Thus, we can conclude that after a moderate number of time intervals, CoSLAS compensates for the lack of perfect knowledge of the clock or location-related parameters.

In Fig. 7, we show the estimated and true trajectories and the RMSEs versus time n for $Q = 1$ and $Q = 5$. It is seen that at early times, the location RMSE is higher for $Q = 1$ than for $Q = 5$. The increased location RMSE around time $n = 10$ can be explained as before. The clock RMSE is generally higher for $Q = 1$ since the clock information provided by the temporal reference agents cannot be disseminated throughout the network during one message passing iteration, and hence (because $Q = 1$) during one time step. However, the location-related RMSEs suggest that the local synchronicity between neighboring agents is sufficient for obtaining accurate location-related estimates. The fluctuation of the clock RMSEs is caused by the time-varying network connectivity and the random-walk evolution model (2). Finally, the performance of CoSLAS is again generally close to that of ClkRef and LocRef.

We assessed the computational complexity of the proposed CoSLAS algorithm by measuring runtimes of our Matlab implementation (R2010b) on an Intel Core i5 CPU. We note that our Matlab code is not optimized for runtime and includes some overhead to simulate network interactions. For the con-

[2]This relation between the number of message passing iterations needed for convergence and the maximum hop distance to reference agents has been observed also individually for pure localization [21] and pure synchronization [26]. Further results (not shown here) confirm that this relation continues to hold true for CoSLAS in larger networks.

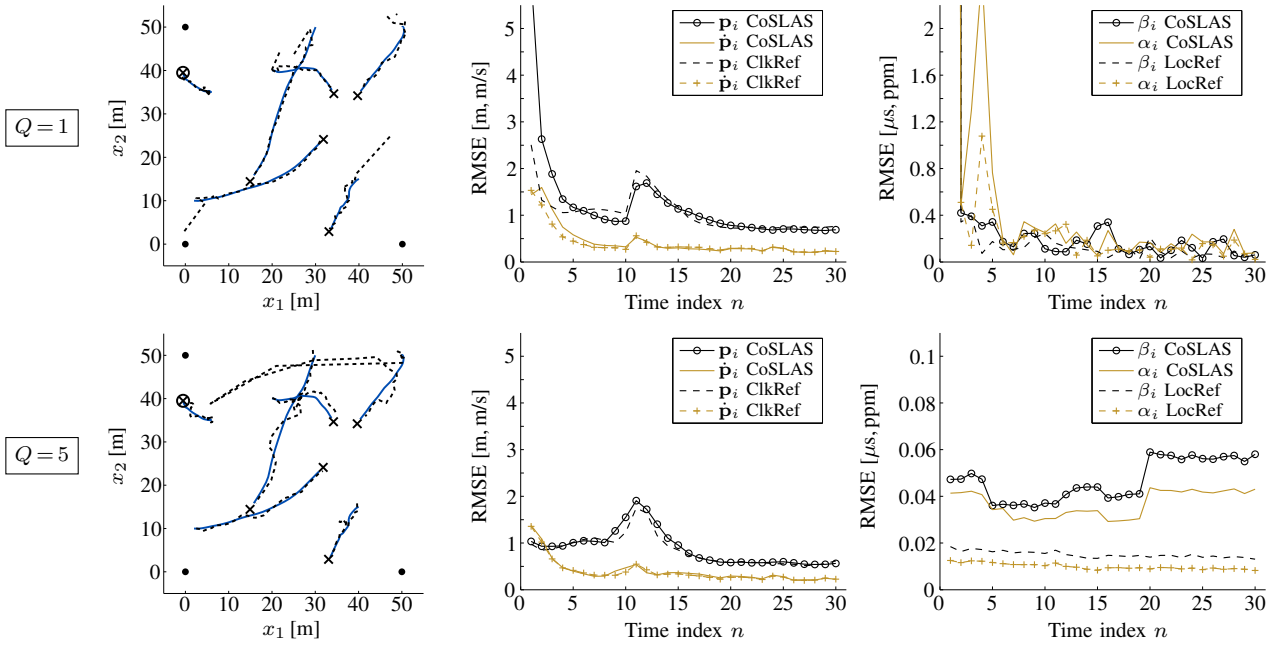

Fig. 7. Trajectories and RMSEs for $Q=1$ (top) and $Q=5$ (bottom). In the leftmost figures, solid blue lines indicate the true trajectories and dashed black lines the estimated trajectories.

sidered scenario, and with the number of particles $\left|\mathcal{T}_i^{p(q)}\right|L$ chosen as 1000, 1500, 2000, and 2500, the average runtime per agent i and iteration q was measured as 0.130 s, 0.147 s, 0.158 s, and 0.181 s, respectively. However, using more than 1000 particles did not improve the estimation accuracy.

VIII. Conclusion

We presented a distributed, sequential belief propagation (BP) algorithm for cooperative simultaneous localization and synchronization (CoSLAS) in mobile, decentralized agent networks with time-varying clocks. The agents acquire interagent distance estimates from time-of-flight measurements. We exploited the resulting close relation between localization and synchronization to establish a common statistical formulation that features a conditional independence of time measurements and location-related parameters given the interagent distances. This independence is leveraged by the proposed BP algorithm to obtain reduced dimensions of the messages and thus a reduced complexity. The combined use of particle representations and parametric representations leads to high accuracy at low communication cost, and a judiciously chosen message schedule allows for real-time operation in networks with rapidly changing connectivity. Simulation results demonstrated the good performance of the proposed algorithm in a challenging scenario with only one temporal reference agent and time-varying network connectivity.

Possible directions of future work include the use of computationally efficient BP variants such as sigma-point BP [24] or mean field message passing [40] to reduce the computational complexity of the nonparametric message operations, and the consideration of alternative factorizations to obtain simpler message representations. Furthermore, the use of more accurate clock and measurement models [41], [42] and the inclusion of non-line-of-sight mitigation [43] can be expected to result in a performance improvement. Finally, an extension of the proposed BP algorithm including the estimation of hyperparameters, such as the measurement noise variance σ_v^2, would be of interest [44].

Appendix A

We derive the parameter updates presented in Section VI-A (eqs. (27)–(32)), Section VI-B1 (eqs. (33), (34)), and Section VI-B3 (eqs. (37), (38)). For some covariance matrix $\mathbf{\Sigma}$ and two nonzero matrices $\mathbf{A}$ and $\mathbf{B}$, consider the function $f(\mathbf{z}_1,\mathbf{z}_2)=\exp\left(-\frac{1}{2}\|\mathbf{A}\mathbf{z}_1+\mathbf{B}\mathbf{z}_2\|_{\mathbf{\Sigma}}^2\right)$. Given $\eta(\mathbf{z}_1)\propto\mathcal{N}\left(\mathbf{z}_1;\boldsymbol{\mu}_1,\mathbf{\Sigma}_1\right)$, we calculate the message $\zeta(\mathbf{z}_2)$ according to (23), specialized to the case where $\eta(\mathbf{z}_1)$ is the only message in the product in (23). We obtain [26]

$$\begin{aligned}
&\zeta(\mathbf{z}_2)\\
&=\int f(\mathbf{z}_1,\mathbf{z}_2)\,\eta(\mathbf{z}_1)\,\mathrm{d}\mathbf{z}_1\\
&\propto\int\exp\Bigg(-\frac{1}{2}\big(\mathbf{z}_2^{\mathrm{T}}\mathbf{B}^{\mathrm{T}}\mathbf{\Sigma}^{-1}\mathbf{B}\mathbf{z}_2+\mathbf{z}_1^{\mathrm{T}}(\mathbf{A}^{\mathrm{T}}\mathbf{\Sigma}^{-1}\mathbf{A}+\mathbf{\Sigma}_1^{-1})\mathbf{z}_1\\
&\qquad-2\mathbf{z}_1^{\mathrm{T}}(\mathbf{A}^{\mathrm{T}}\mathbf{\Sigma}^{-1}\mathbf{B}\mathbf{z}_2+\mathbf{\Sigma}_1^{-1}\boldsymbol{\mu}_1)+\boldsymbol{\mu}_1^{\mathrm{T}}\mathbf{\Sigma}_1^{-1}\boldsymbol{\mu}_1\big)\Bigg)\mathrm{d}\mathbf{z}_1\\
&\propto\exp\left(-\frac{1}{2}\|\mathbf{z}_2-\boldsymbol{\mu}_2\|_{\mathbf{\Sigma}_2}^2\right),
\end{aligned}$$

where

$$\begin{aligned}
\mathbf{\Sigma}_2&\triangleq\big(\mathbf{B}^{\mathrm{T}}\mathbf{\Sigma}^{-1}\mathbf{B}-\mathbf{B}^{\mathrm{T}}\mathbf{\Sigma}^{-1}\mathbf{A}(\mathbf{A}^{\mathrm{T}}\mathbf{\Sigma}^{-1}\mathbf{A}+\mathbf{\Sigma}_1^{-1})^{-1}\\
&\qquad\times\mathbf{A}^{\mathrm{T}}\mathbf{\Sigma}^{-1}\mathbf{B}\big)^{-1},\qquad(46)\\
\boldsymbol{\mu}_2&\triangleq\mathbf{\Sigma}_2\mathbf{B}^{\mathrm{T}}\mathbf{\Sigma}^{-1}\mathbf{A}(\mathbf{A}^{\mathrm{T}}\mathbf{\Sigma}^{-1}\mathbf{A}+\mathbf{\Sigma}_1^{-1})^{-1}\mathbf{\Sigma}_1^{-1}\boldsymbol{\mu}_1\,.\qquad(47)
\end{aligned}$$

The parameter updates in (33), (34) and in (37), (38) are now obtained by reformulating (46), (47) using the relevant vectors and matrices. More

specifically, we set $(\boldsymbol{\mu}_1, \boldsymbol{\mu}_2, \mathbf{A}, \mathbf{B}, \boldsymbol{\Sigma}, \boldsymbol{\Sigma}_1, \boldsymbol{\Sigma}_2)$ to $(\boldsymbol{\mu}^{(q)}_{j\to i,1}, \mu^{(q)}_{f_{ij}\to d_{ij}}, \mathbf{D}_{ij}, \mathbf{a}_d, \mathbf{I}, \boldsymbol{\Sigma}^{(q)}_{j\to i,1}, \sigma^{2\,(q)}_{f_{ij}\to d_{ij}})$ for (33), (34) and to $(\boldsymbol{\mu}^{(q)}_{j\to i,2}, \boldsymbol{\mu}^{(q)}_{f_{ij}\to\vartheta_i}, \mathbf{C}_{ij}, \mathbf{A}_{ij}, \mathbf{I}, \boldsymbol{\Sigma}^{(q)}_{j\to i,2}, \boldsymbol{\Sigma}^{(q)}_{f_{ij}\to\vartheta_i})$ for (37). (38). For the parameter updates in the prediction step in Section VI-A, we have $\mathbf{B}=\mathbf{I}$ in (46), (47). By applying Woodbury's identity [45], eqs. (46), (47) then simplify to

$$\boldsymbol{\Sigma}_2 = \mathbf{A}\boldsymbol{\Sigma}_1\mathbf{A}^{\mathrm{T}} + \boldsymbol{\Sigma}\,, \qquad \boldsymbol{\mu}_2 = \mathbf{A}\boldsymbol{\mu}_1\,. \tag{48}$$

Then, (27)–(32) are obtained by reformulating (48) using the relevant vectors and matrices. More specifically, we set $(\boldsymbol{\mu}_1, \boldsymbol{\mu}_2, \mathbf{A}, \boldsymbol{\Sigma}, \boldsymbol{\Sigma}_1, \boldsymbol{\Sigma}_2)$ to $(\boldsymbol{\mu}^{-}_{\vartheta_i\to f_i}, \boldsymbol{\mu}_{f_i\to\vartheta_i}, \mathbf{I}, \boldsymbol{\Sigma}_{u_{1,i}}, \boldsymbol{\Sigma}^{-}_{\vartheta_i\to f_i}, \boldsymbol{\Sigma}_{f_i\to\vartheta_i})$ for (27), (28); to $(\boldsymbol{\mu}^{-}_{x_i\to l_i,s}, \boldsymbol{\mu}_{l_i\to x_i,s}, \mathbf{G}_1, \boldsymbol{\Sigma}_{u_{2,i}}, \boldsymbol{\Sigma}^{-}_{x_i\to l_i,s}, \boldsymbol{\Sigma}_{l_i\to x_i,s})$ for (29), (30); and to $(\boldsymbol{\mu}_{l_i\to x_i,s}, \boldsymbol{\mu}_{\psi_i\to\tilde{p}_i,s}, \mathbf{P}, \mathbf{0}, \boldsymbol{\Sigma}_{l_i\to x_i,s}, \boldsymbol{\Sigma}_{\psi_i\to\tilde{p}_i,s})$ for (31), (32).

Appendix B

We derive the Gaussian approximation of $\zeta^{(q)}_{\phi_{ij}}(d_{ij})$ presented in Section VI-B2. According to (23), we have

$$\zeta^{(q)}_{\phi_{ij}}(d_{ij}) = \iint \phi_{ij}\, \eta^{(q-1)}_{\phi_{ij}}(\tilde{\mathbf{p}}_i)\, \eta^{(q-1)}_{\phi_{ji}}(\tilde{\mathbf{p}}_j)\, \mathrm{d}\tilde{\mathbf{p}}_i \mathrm{d}\tilde{\mathbf{p}}_j\,,$$

with $\phi_{ij} = \delta\big(\|\tilde{\mathbf{p}}_i - \tilde{\mathbf{p}}_j\| - d_{ij}\big)$. Inserting the Gaussian mixture representations of $\eta^{(q-1)}_{\phi_{ij}}(\tilde{\mathbf{p}}_i)$ and $\eta^{(q-1)}_{\phi_{ji}}(\tilde{\mathbf{p}}_j)$ (cf. Table II) gives

$$\zeta^{(q)}_{\phi_{ij}}(d_{ij}) = \sum_{r=1}^{S^{(q-1)}_{i\to j}} \sum_{s=1}^{S^{(q-1)}_{j\to i}} w^{(q-1)}_{i\to j,r}\, w^{(q-1)}_{j\to i,s}\, \Psi_{ij,rs}(d_{ij}), \tag{49}$$

where

$$\begin{aligned}\Psi_{ij,rs}(d_{ij}) &\triangleq \iint \delta\big(\|\tilde{\mathbf{p}}_{i,r} - \tilde{\mathbf{p}}_{j,s}\| - d_{ij}\big)\, \mathcal{N}\big(\tilde{\mathbf{p}}_{i,r}; \boldsymbol{\mu}^{(q-1)}_{\tilde{p}_i\to\phi_{ij},r}, \boldsymbol{\Sigma}^{(q-1)}_{\tilde{p}_i\to\phi_{ij},r}\big) \\ &\qquad \times \mathcal{N}\big(\tilde{\mathbf{p}}_{j,s}; \boldsymbol{\mu}^{(q-1)}_{\tilde{p}_j\to\phi_{ji},s}, \boldsymbol{\Sigma}^{(q-1)}_{\tilde{p}_j\to\phi_{ji},s}\big)\, \mathrm{d}\tilde{\mathbf{p}}_{i,r}\, \mathrm{d}\tilde{\mathbf{p}}_{j,s}\,. \end{aligned}\tag{50}$$

Here, $\Psi_{ij,rs}(d_{ij})$ describes the (r,s)th Gaussian mixture component and, e.g., $\tilde{\mathbf{p}}_{i,r} \sim \mathcal{N}\big(\tilde{\mathbf{p}}_{i,r}; \boldsymbol{\mu}^{(q-1)}_{\tilde{p}_i\to\phi_{ij},r}, \boldsymbol{\Sigma}^{(q-1)}_{\tilde{p}_i\to\phi_{ij},r}\big)$ corresponds to the rth Gaussian component. We can write $d_{ij} = \|\tilde{\mathbf{p}}_{i,r} - \tilde{\mathbf{p}}_{j,s}\|$ as a function $d_{ij} = \chi(\tilde{\mathbf{p}}_{ij,rs})$ of the stacked vector $\tilde{\mathbf{p}}_{ij,rs} \triangleq \big[\tilde{\mathbf{p}}^{\mathrm{T}}_{i,r}\ \tilde{\mathbf{p}}^{\mathrm{T}}_{j,s}\big]^{\mathrm{T}}$. We have $\tilde{\mathbf{p}}_{ij,rs} \sim f(\tilde{\mathbf{p}}_{ij,rs}) = \mathcal{N}(\tilde{\mathbf{p}}_{ij,rs}; \boldsymbol{\mu}_{ij,rs}, \boldsymbol{\Sigma}_{ij,rs})$, where $\boldsymbol{\mu}_{ij,rs} \triangleq \big[\boldsymbol{\mu}^{(q-1)\mathrm{T}}_{\tilde{p}_i\to\phi_{ij},r}\ \ \boldsymbol{\mu}^{(q-1)\mathrm{T}}_{\tilde{p}_j\to\phi_{ji},s}\big]^{\mathrm{T}}$ and $\boldsymbol{\Sigma}_{ij,rs}$ has been specified in Section VI-B2; furthermore, $\mathcal{N}\big(\tilde{\mathbf{p}}_{i,r}; \boldsymbol{\mu}^{(q-1)}_{\tilde{p}_i\to\phi_{ij},r}, \boldsymbol{\Sigma}^{(q-1)}_{\tilde{p}_i\to\phi_{ij},r}\big)\mathcal{N}\big(\tilde{\mathbf{p}}_{j,s}; \boldsymbol{\mu}^{(q-1)}_{\tilde{p}_j\to\phi_{ji},s}, \boldsymbol{\Sigma}^{(q-1)}_{\tilde{p}_j\to\phi_{ji},s}\big) = \mathcal{N}(\tilde{\mathbf{p}}_{ij,rs}; \boldsymbol{\mu}_{ij,rs}, \boldsymbol{\Sigma}_{ij,rs})$. Therefore, we can rewrite (50) as

$$\Psi_{ij,rs}(d_{ij}) = \int \delta\big(\chi(\tilde{\mathbf{p}}_{ij,rs}) - d_{ij}\big)\, \mathcal{N}(\tilde{\mathbf{p}}_{ij,rs}; \boldsymbol{\mu}_{ij,rs}, \boldsymbol{\Sigma}_{ij,rs})\, \mathrm{d}\tilde{\mathbf{p}}_{ij,rs}. \tag{51}$$

For an approximate evaluation of this integral, we linearize the function $\chi(\tilde{\mathbf{p}}_{ij,rs})$ around $\boldsymbol{\mu}_{ij,rs}$. This yields

$$\begin{aligned}&\chi(\tilde{\mathbf{p}}_{ij,rs}) \\ &\approx \tilde{\chi}_{rs}(\tilde{\mathbf{p}}_{ij,rs}) \triangleq \big\|\boldsymbol{\mu}^{(q-1)}_{d_{ij},rs}\big\| + \bar{\boldsymbol{\mu}}^{(q-1)\mathrm{T}}_{d_{ij},rs}(\tilde{\mathbf{p}}_{ij,rs} - \boldsymbol{\mu}_{ij,rs}),\end{aligned}\tag{52}$$

with $\boldsymbol{\mu}^{(q-1)}_{d_{ij},rs}$ and $\bar{\boldsymbol{\mu}}^{(q-1)}_{d_{ij},rs}$ as defined in Section VI-B2. Inserting (52) into (51), we obtain the approximation

$$\begin{aligned}&\Psi_{ij,rs}(d_{ij}) \\ &\approx \tilde{\Psi}_{ij,rs}(d_{ij}) \\ &\triangleq \int \delta\big(\tilde{\chi}_{rs}(\tilde{\mathbf{p}}_{ij,rs}) - d_{ij}\big)\, \mathcal{N}(\tilde{\mathbf{p}}_{ij,rs}; \boldsymbol{\mu}_{ij,rs}, \boldsymbol{\Sigma}_{ij,rs})\, \mathrm{d}\tilde{\mathbf{p}}_{ij,rs}\,.\end{aligned}\tag{53}$$

Within our approximation $d_{ij} \approx \tilde{\chi}_{rs}(\tilde{\mathbf{p}}_{ij,rs})$, $\delta\big(\tilde{\chi}_{rs}(\tilde{\mathbf{p}}_{ij,rs}) - d_{ij}\big)$ can be interpreted as $f(d_{ij}|\tilde{\mathbf{p}}_{ij,rs})$. Hence, (53) becomes

$$\tilde{\Psi}_{ij,rs}(d_{ij}) = \int f(d_{ij}|\tilde{\mathbf{p}}_{ij,rs})\, f(\tilde{\mathbf{p}}_{ij,rs})\, \mathrm{d}\tilde{\mathbf{p}}_{ij,rs} = f_{rs}(d_{ij}), \tag{54}$$

where $f_{rs}(d_{ij})$ denotes the pdf of d_{ij} under our approximation $d_{ij} \approx \tilde{\chi}_{rs}(\tilde{\mathbf{p}}_{ij,rs})$. Because $f(\tilde{\mathbf{p}}_{ij,rs}) = \mathcal{N}(\tilde{\mathbf{p}}_{ij,rs}; \boldsymbol{\mu}_{ij,rs}, \boldsymbol{\Sigma}_{ij,rs})$ and $\tilde{\chi}_{rs}(\cdot)$ is an affine function (see (52)), $f_{rs}(d_{ij})$ is again Gaussian, i.e., $f_{rs}(d_{ij}) = \mathcal{N}\big(d_{ij}; \mu_{d,rs}, \sigma^2_{d,rs}\big)$, with

$$\begin{aligned}\mu_{d,rs} &= \mathbb{E}[\tilde{\chi}_{rs}(\tilde{\mathbf{p}}_{ij,rs})] \\ &= \big\|\boldsymbol{\mu}^{(q-1)}_{d_{ij},rs}\big\| + \bar{\boldsymbol{\mu}}^{(q-1)\mathrm{T}}_{d_{ij},rs}\big(\mathbb{E}[\tilde{\mathbf{p}}_{ij,rs}] - \boldsymbol{\mu}_{ij,rs}\big) \\ &= \big\|\boldsymbol{\mu}^{(q-1)}_{d_{ij},rs}\big\|\end{aligned}$$

and

$$\begin{aligned}\sigma^2_{d,rs} &= \mathrm{var}[\tilde{\chi}_{rs}(\tilde{\mathbf{p}}_{ij,rs})] \\ &= \bar{\boldsymbol{\mu}}^{(q-1)\mathrm{T}}_{d_{ij},rs}\, \mathrm{cov}[\tilde{\mathbf{p}}_{ij,rs} - \boldsymbol{\mu}_{ij,rs}]\, \bar{\boldsymbol{\mu}}^{(q-1)}_{d_{ij},rs} \\ &= \bar{\boldsymbol{\mu}}^{(q-1)\mathrm{T}}_{d_{ij},rs}\, \boldsymbol{\Sigma}_{ij,rs}\, \bar{\boldsymbol{\mu}}^{(q-1)}_{d_{ij},rs}.\end{aligned}$$

Thus, because of (54), we also have $\tilde{\Psi}_{ij,rs}(d_{ij}) = \mathcal{N}\big(d_{ij}; \mu_{d,rs}, \sigma^2_{d,rs}\big)$. Substituting this for $\Psi_{ij,rs}(d_{ij})$ in (49) yields

$$\zeta^{(q)}_{\phi_{ij}}(d_{ij}) \approx \sum_{r=1}^{S^{(q-1)}_{i\to j}} \sum_{s=1}^{S^{(q-1)}_{j\to i}} w^{(q-1)}_{i\to j,r}\, w^{(q-1)}_{j\to i,s}\, \mathcal{N}\big(d_{ij}; \mu_{d,rs}, \sigma^2_{d,rs}\big).$$

This is a mixture of up to four Gaussian components. Finally, we use moment matching [46] to approximate this Gaussian mixture by a single Gaussian. The resulting mean and variance are given in (35) and (36), respectively.

Acknowledgment

The authors would like to thank the anonymous reviewers, whose comments led to an improvement of this paper.

References

[1] P. Corke, T. Wark, R. Jurdak, W. Hu, P. Valencia, and D. Moore, "Environmental wireless sensor networks," *Proc. IEEE*, vol. 98, pp. 1903–1917, Nov. 2010.

[2] T. Zhao and A. Nehorai, "Distributed sequential Bayesian estimation of a diffusive source in wireless sensor networks," *IEEE Trans. Signal Process.*, vol. 55, pp. 1511–1524, Apr. 2007.

[3] J. Ko, C. Lu, M. B. Srivastava, J. A. Stankovic, A. Terzis, and M. Welsh, "Wireless sensor networks for healthcare," *Proc. IEEE*, vol. 98, pp. 1947–1960, Nov. 2010.

[4] R. Di Taranto, L. S. Muppirisetty, R. Raulefs, D. Slock, T. Svensson, and H. Wymeersch, "Location-aware communications for 5G networks: How location information can improve scalability, latency, and robustness of 5G," *IEEE Signal Process. Mag.*, vol. 31, pp. 102–112, Nov. 2014.

[5] N. Patwari, J. N. Ash, S. Kyperountas, A. O. Hero III, R. L. Moses, and N. S. Correal, "Locating the nodes: Cooperative localization in wireless sensor networks," *IEEE Signal Process. Mag.*, vol. 22, pp. 54–69, Jul. 2005.

[6] S. Zhu and Z. Ding, "Joint synchronization and localization using TOAs: A linearization based WLS solution," *IEEE J. Sel. Areas Commun.*, vol. 28, pp. 1017–1025, Aug. 2010.

[7] S. P. Chepuri, G. Leus, and A.-J. van der Veen, "Joint localization and clock synchronization for wireless sensor networks," in *Proc. Asilomar Conf. Sig., Syst., Comput.*, Pacific Grove, CA, USA, pp. 1432–1436, Nov. 2012.

[8] Y. Wang, X. Ma, and G. Leus, "Robust time-based localization for asynchronous networks," *IEEE Trans. Signal Process.*, vol. 59, pp. 4397–4410, Sep. 2011.

[9] J. Zheng and Y.-C. Wu, "Joint time synchronization and localization of an unknown node in wireless sensor networks," *IEEE Trans. Signal Process.*, vol. 58, pp. 1309–1320, Mar. 2010.

[10] D. Zachariah, A. De Angelis, S. Dwivedi, and P. Händel, "Schedule-based sequential localization in asynchronous wireless networks," *EURASIP J. Adv. Signal Process.*, vol. 16, pp. 1–12, Dec. 2014.

[11] R. M. Vaghefi and R. M. Buehrer, "Cooperative joint synchronization and localization in wireless sensor networks," *IEEE Trans. Signal Process.*, vol. 63, pp. 3615–3627, Jul. 2015.

[12] A. Yeredor, "Decentralized TOA-based localization in non-synchronized wireless networks with partial, asymmetric connectivity," in *Proc. IEEE SPAWC-14*, Toronto, Canada, pp. 165–169, Jun. 2014.

[13] D. Benoît, J.-B. Pierrot, and C. Abou-Rjeily, "Joint distributed synchronization and positioning in UWB ad hoc networks using TOA," *IEEE Trans. Microw. Theory Techn.*, vol. 54, pp. 1896–1911, Apr. 2006.

[14] F. Meyer, B. Etzlinger, F. Hlawatsch, and A. Springer, "A distributed particle-based belief propagation algorithm for cooperative simultaneous localization and synchronization," in *Proc. Asilomar Conf. Sig., Syst., Comput.*, Pacific Grove, CA, USA, pp. 527–531, Nov. 2013.

[15] B. Etzlinger, F. Meyer, A. Springer, F. Hlawatsch, and H. Wymeersch, "Cooperative simultaneous localization and synchronization: A distributed hybrid message passing algorithm," in *Proc. Asilomar Conf. Sig., Syst., Comput.*, Pacific Grove, CA, USA, pp. 1978–1982, Nov. 2013.

[16] W. Yuan, N. Wu, H. Wang, B. Li, and J. Kuang, "Variational message passing for joint localization and synchronization in wireless sensor networks," in *Proc. IEEE/CIC ICCC-14*, Shanghai, China, pp. 437–441, Oct. 2014.

[17] A. Ahmad, E. Serpedin, H. Nounou, and M. Nounou, "Joint node localization and time-varying clock synchronization in wireless sensor networks," *IEEE Trans. Wireless Commun.*, vol. 12, pp. 5322–5333, Oct. 2013.

[18] J. Li and A. Nehorai, "Joint sequential target estimation and clock synchronization in wireless sensor networks," *IEEE Trans. Signal Inf. Process. Netw.*, vol. 1, pp. 74–88, June 2015.

[19] W. Yuan, N. Wu, B. Etzlinger, H. Wang, B. Li, and J. Kuang, "Cooperative joint localization and clock synchronization based on Gaussian message passing in asynchronous wireless networks," *IEEE Trans. Veh. Technol.*, vol. 65, pp. 7258–7273, Sept. 2016.

[20] B. Etzlinger, F. Meyer, H. Wymeersch, F. Hlawatsch, A. Springer, and G. Müller, "Cooperative simultaneous localization and synchronization: Toward a low-cost hardware implementation," in *Proc. IEEE SAM-14*, A Coruña, Spain, pp. 33–36, June 2014.

[21] A. T. Ihler, J. W. Fisher, R. L. Moses, and A. S. Willsky, "Nonparametric belief propagation for self-localization of sensor networks," *IEEE J. Sel. Areas Commun.*, vol. 23, pp. 809–819, Apr. 2005.

[22] H. Wymeersch, J. Lien, and M. Z. Win, "Cooperative localization in wireless networks," *Proc. IEEE*, vol. 97, pp. 427–450, Feb. 2009.

[23] M. A. Caceres, F. Penna, H. Wymeersch, and R. Garello, "Hybrid cooperative positioning based on distributed belief propagation," *IEEE J. Sel. Areas Commun.*, vol. 29, pp. 1948–1958, Dec. 2011.

[24] F. Meyer, O. Hlinka, and F. Hlawatsch, "Sigma point belief propagation," *IEEE Signal Process. Lett.*, vol. 21, pp. 145–149, Feb. 2014.

[25] T. Lv, H. Gao, X. Li, S. Yang, and L. Hanzo, "Space-time hierarchical-graph based cooperative localization in wireless sensor networks," *IEEE Trans. Signal Process.*, vol. 64, pp. 322–334, Jan. 2016.

[26] B. Etzlinger, H. Wymeersch, and A. Springer, "Cooperative synchronization in wireless networks," *IEEE Trans. Signal Process.*, vol. 62, pp. 2837–2849, June 2014.

[27] F. Meyer, O. Hlinka, H. Wymeersch, E. Riegler, and F. Hlawatsch, "Distributed localization and tracking of mobile networks including noncooperative objects," *IEEE Trans. Signal Inf. Process. Netw.*, vol. 2, pp. 57–71, Mar. 2016.

[28] H.-A. Loeliger, J. Dauwels, J. Hu, S. Korl, L. Ping, and F. R. Kschischang, "The factor graph approach to model-based signal processing," *Proc. IEEE*, vol. 95, pp. 1295–1322, June 2007.

[29] M. J. Wainwright and M. I. Jordan, "Graphical models, exponential families, and variational inference," *Found. Trends Mach. Learn.*, vol. 1, pp. 1–305, Jan. 2008.

[30] H. Wymeersch, *Iterative Receiver Design*. Cambridge, UK: Cambridge University Press, 2007.

[31] T. Sathyan and M. Hedley, "Fast and accurate cooperative tracking in wireless networks," *IEEE Trans. Mobile Comput.*, vol. 12, pp. 1801–1813, Sep. 2013.

[32] S. P. Chepuri, R. T. Rajan, G. Leus, and A.-J. van der Veen, "Joint clock synchronization and ranging: Asymmetrical time-stamping and passive listening," *IEEE Signal Process. Lett.*, vol. 20, pp. 51–54, Jan. 2013.

[33] S. M. Kay, *Fundamentals of Statistical Signal Processing: Estimation Theory*. Upper Saddle River, NJ: Prentice-Hall, 1993.

[34] K. Das and H. Wymeersch, "Censoring for Bayesian cooperative positioning in dense wireless networks," *IEEE J. Sel. Areas Commun.*, vol. 30, pp. 1835–1842, Oct. 2012.

[35] F. Meyer, F. Hlawatsch, and H. Wymeersch, "Cooperative simultaneous localization and tracking (CoSLAT) with reduced complexity and communication," in *Proc. IEEE ICASSP-13*, Vancouver, Canada, pp. 4484–4488, May 2013.

[36] A. Doucet, N. de Freitas, and N. Gordon, *Sequential Monte Carlo Methods in Practice*. New York, NY, USA: Springer, 2001.

[37] G. Gan, C. Ma, and J. Wu, *Data Clustering: Theory, Algorithms, and Applications*. Philadelphia, PA, USA: SIAM, 2007.

[38] D. M. Malioutov, J. K. Johnson, and A. S. Willsky, "Walk-sums and belief propagation in Gaussian graphical models," *J. Machine Learn. Res.*, vol. 7, pp. 2031–2064, 2006.

[39] V. Savic and H. Wymeersch, "Simultaneous localization and tracking via real-time nonparametric belief propagation," in *Proc. IEEE ICASSP-13*, Vancouver, Canada, pp. 5180–5184, May 2013.

[40] B. Etzlinger, D. Bartel, W. Haselmayr, and A. Springer, "Mean field message passing for cooperative simultaneous ranging and synchronization," in *Proc. IEEE Global Conf. Sig. Inf. Process.*, Austin, TX, USA, pp. 583–586, Dec. 2013.

[41] R. T. Rajan and A. J. van der Veen, "Joint ranging and synchronization for an anchorless network of mobile nodes," *IEEE Trans. Signal Process.*, vol. 63, pp. 1925–1940, Apr. 2015.

[42] B. Etzlinger, N. Palaoro, W. Haselmayr, B. Rudic, and A. Springer, "Timestamp free synchronization with sub-tick accuracy in the presence of discrete clocks," *IEEE Trans. Wireless Commun.*, vol. 16, pp. 771–783, Feb. 2017.

[43] S. Van de Velde, G. Abreu, and H. Steendam, "Improved censoring and NLOS avoidance for wireless localization in dense networks," *IEEE J. Sel. Areas Commun.*, vol. 33, pp. 2302–2312, Nov. 2015.

[44] F. Meyer, P. Braca, F. Hlawatsch, M. Micheli, and K. LePage, "Scalable adaptive multitarget tracking using multiple sensors," in *Proc. IEEE GLOBECOM-16*, Washington D.C., USA, Dec. 2016.

[45] K. B. Petersen and M. S. Pedersen, "The Matrix Cookbook," Nov. 2012. available online: http://www2.imm.dtu.dk/pubdb/p.php?3274.

[46] U. Orguner and M. Demirekler, "Analysis of single Gaussian approximation of Gaussian mixtures in Bayesian filtering applied to mixed multiple-model estimation," *Int. J. Control*, vol. 80, pp. 952–967, July 2007.

Bernhard Etzlinger (S'11–M'16) received the Dipl.-Ing. (M.Sc.) degree in mechatronics in 2010 and the Dr. techn. (Ph.D.) degree in technical sciences in 2016, both from Johannes Kepler University Linz, Linz, Austria. In 2010, he worked at Fraunhofer FKIE, Wachtberg, Germany. During his Ph.D. studies, he was a visiting student with the Department of Signals and Systems, Chalmers University of Technology, Gothenburg, Sweden, and with the Department of Electrical and Computer Engineering, Texas A&M University, College Station, TX, USA. His research activities are focused on statistical signal processing for receiver design, and cooperative network clock synchronization and localization.

Florian Meyer (S'12–M'15) received the Dipl.-Ing. (M.Sc.) and Ph.D. degrees in electrical engineering from TU Wien, Vienna, Austria in 2011 and 2015, respectively. From 2011 to 2016, he was a Research and Teaching Assistant with the Institute of Telecommunications, TU Wien. He was a visiting student at the Department of Signals and Systems, Chalmers University of Technology, Gothenburg, Sweden in 2013 and at the Centre of Maritime Research and Experimentation (CMRE), La Spezia, Italy in 2014 and 2015. He joined CMRE as a scientist in 2016. Dr. Meyer is currently a Postdoctoral Fellow with the Laboratory for Information and Decision Systems (LIDS) at the Massachusetts Institute of Technology (MIT), Cambridge, MA, USA and on leave of absence from CMRE. His research interests include signal processing for wireless sensor networks, localization and tracking, information-seeking control, message passing algorithms, and finite set statistics.

Franz Hlawatsch (S'85–M'88–SM'00–F'12) received the Diplom-Ingenieur, Dr. techn., and Univ.-Dozent (habilitation) degrees in electrical engineering/signal processing from TU Wien, Vienna, Austria in 1983, 1988, and 1996, respectively. Since 1983, he has been with the Institute of Telecommunications, TU Wien, where he is currently an Associate Professor. During 1991–1992, as a recipient of an Erwin Schrödinger Fellowship, he spent a sabbatical year with the Department of Electrical Engineering, University of Rhode Island, Kingston, RI, USA. In 1999, 2000, and 2001, he held one-month Visiting Professor positions with INP/ENSEEIHT, Toulouse, France and IRCCyN, Nantes, France. He (co)authored a book, three review papers that appeared in the IEEE SIGNAL PROCESSING MAGAZINE, about 200 refereed scientific papers and book chapters, and three patents. He coedited three books. He was Technical Program Co-Chair of EUSIPCO 2004 and served on the technical committees of numerous IEEE conferences. He was an Associate Editor for the IEEE TRANSACTIONS ON SIGNAL PROCESSING from 2003 to 2007 and for the IEEE TRANSACTIONS ON INFORMATION THEORY from 2008 to 2011. From 2004 to 2009, he was a member of the IEEE SPCOM Technical Committee. He currently serves as an Associate Editor for the IEEE TRANSACTIONS ON SIGNAL AND INFORMATION PROCESSING OVER NETWORKS. He coauthored papers that won an IEEE Signal Processing Society Young Author Best Paper Award and a Best Student Paper Award at IEEE ICASSP 2011. His research interests include statistical and compressive signal processing methods and their application to sensor networks and wireless communications.

Andreas Springer (S'90–A'97–M'99) received the Dipl.-Ing. degree in Electrical Engineering from TU Wien, Vienna, Austria, in 1991, and the Dr. techn. (Ph.D) and Univ.-Doz. (Habilitation) degrees from the Johannes Kepler University Linz (JKU), Linz, Austria in 1996 and 2001, respectively. From 1991 to 1996, he was with the Microelectronics Institute at JKU. In 1997, he joined the Institute for Communications and Information Engineering at the same university, where he became a full professor in 2005. Since July 2002, he has been head of the Institute for Communications Engineering and RF-Systems (formerly Institute for Communications and Information Engineering) at JKU. He serves as the coordinator for the research area "Wireless Systems" in the Austrian Center of Competence in Mechatronics (ACCM). He is a member of the editorial board of the International Journal of Electronics and Communications, and he serves as a reviewer for a number of international journals and conferences. He has been engaged in research work on GaAs integrated millimeter-wave TEDs, MMICs and millimeter-wave sensor systems. His current research interests are focused on wireless communication systems, architectures and algorithms for multi-band/multi-mode transceivers, wireless sensor networks, millimeter wave communications, and recently molecular communications. In these fields, he has published more than 200 papers in journals and at international conferences, one book, and two book chapters. In 2006, he was co-recipient of the science prize of the German Aerospace Center (DLR). Dr. Springer is a member of the IEEE Microwave Theory and Techniques Society, the IEEE Communications Society, the IEEE Vehicular Technology Society, OVE, and VDI. From 2002 to 2012, he served as Chair of the IEEE Austrian Joint COM/MTT Chapter.

Henk Wymeersch (S'01–M'05) obtained the Ph.D. degree in Electrical Engineering/Applied Sciences in 2005 from Ghent University, Belgium. He is currently a Professor of Communication Systems with the Department of Signals and Systems at Chalmers University of Technology, Sweden. Prior to joining Chalmers, he was a postdoctoral researcher from 2005 until 2009 with the Laboratory for Information and Decision Systems at the Massachusetts Institute of Technology. Prof. Wymeersch served as Associate Editor for IEEE Communication Letters (2009–2013), IEEE Transactions on Wireless Communications (since 2013), and IEEE Transactions on Communications (since 2016). His current research interests include cooperative systems and intelligent transportation.